Journal of Mammalian Evolution (2023) 30:923–961
https://doi.org/10.1007/s10914-023-09683-3

RESEARCH

Deinotherium levius and *Tetralophodon longirostris* (Proboscidea, Mammalia) from the Late Miocene hominid locality Hammerschmiede (Bavaria, Germany), and their biostratigraphic significance for the terrestrial faunas of the European Miocene

George E. Konidaris[1,2] · Thomas Lechner[2,3] · Panagiotis Kampouridis[3] · Madelaine Böhme[2,3]

Accepted: 8 August 2023 / Published online: 19 September 2023

Abstract
During the Miocene, proboscideans reached their greatest diversification, and due to their marked evolutionary changes in dental size and morphology, they comprise an important biostratigraphic/biochronological tool. In this article, we study the proboscideans from the Late Miocene hominid locality Hammerschmiede (Germany), whose fossiliferous layers HAM 6, HAM 4 and HAM 5 are dated to 11.42, 11.44 and 11.62 Ma, respectively. The studied material consists of mandibular, tusk and cheek tooth specimens, which are attributed to the deinothere *Deinotherium levius* and the tetralophodont gomphothere *Tetralophodon longirostris*. An almost complete juvenile mandible of *D. levius* was CT-scanned and revealed that the erupting lower tusks represent the permanent ones. The mandible is most possibly associated with a lower deciduous tusk, and therefore these specimens capture the rare, and short in duration, moment of transition between deciduous and permanent lower tusks in fossil proboscideans and represent the first such example in deinotheres. The chronologically well-constrained proboscidean fauna from Hammerschmiede and the examination of other assemblages from European localities indicate that the coexistence of *D. levius* and *T. longirostris* characterizes the late Astaracian–earliest Vallesian, while Hammerschmiede may showcase the transition from the Middle Miocene trilophodont (*Gomphotherium*)-dominated faunas of central Europe to the Late Miocene tetralophodont-dominated ones. Finally, in order to decipher the dietary preferences of the Hammerschmiede *Tetralophodon* we performed dental mesowear angle analysis, which revealed a mixed-feeding diet with an important browsing component, significantly different from the heavily browsing one of *Deinotherium* known from other localities. Such distinct feeding habits between the taxa indicate niche partitioning, which allowed their sympatry.

Keywords Biostratigraphy · Deinotheres · Dental mesowear · Gomphotheres · Tusk replacement

Introduction

The Miocene is the period of the Cenozoic that evidenced the greatest diversity of proboscideans and additionally documents their first wide distribution outside of Africa (Shoshani and Tassy 1996). After their arrival in Europe during the Early Miocene, as part of the complex "Proboscidean Datum Event" (Tassy 1990), deinotheres, gomphotheres, and mammutids formed the proboscidean faunas of this epoch, and by their rapid diversification and expansion, combined with marked evolutionary changes in terms of dental size and morphology, they comprise an important biostratigraphic and biochronological tool for the whole Miocene. However, certain issues remain still partially explored, either due to the rarity of proboscidean discoveries or due to absence of secure (bio)chronological frameworks, that prohibit the recognition of bioevents (e.g., dispersals, extinctions). The latter is particularly obscured because many important specimens/assemblages that play a crucial role in evolutionary schemes and interpretations are part of historical collections lacking stratigraphic control.

✉ George E. Konidaris
georgios.konidaris@uni-tuebingen.de

1 Palaeoanthropology, Institute for Archaeological Sciences, Department of Geosciences, Eberhard Karls University of Tübingen, Rümelinstr. 23, 72070 Tübingen, Germany

2 Senckenberg Centre for Human Evolution and Palaeoenvironment, Tübingen, Germany

3 Terrestrial Palaeoclimatology, Department of Geosciences, Eberhard Karls University of Tübingen, Sigwartstraße 10, 72074 Tübingen, Germany

Here, we present the proboscidean assemblage (deinotheres and tetralophodont gomphotheres) from the faunal-rich and chronologically well-constrained hominid locality of Hammerschmiede (Germany) dated at the very base of the Late Miocene. The aim of the study is (1) to describe and compare the proboscidean dental and mandibular remains, (2) contribute to the taxonomy, evolution, biostratigraphy and palaeoecology of Miocene deinotheriids and gomphotheriids, and (3) add new data on the replacement of deciduous by permanent lower tusks in deinotheriids, a rarely captured moment of transition in fossil proboscideans, based on a mostly complete juvenile mandible.

Fossiliferous locality and geological setting

The active clay-pit of Hammerschmiede is situated in the North Alpine Foreland Basin (NAFB), 5 km north of the city of Kaufbeuren (Fig. 1). It uncovers 25 m of fine-grained fluvial and overbank deposits, including two lignite seams, belonging to the Upper Series lithostratigraphic unit of the Upper Freshwater Molasse (Doppler 1989). Magnetostratigraphic investigations date this succession to the Middle-to-Late Miocene transition (Kirscher et al. 2016). Fossil vertebrates are preserved mainly in fluvial channels (Fig. 2) and two of these channel structures, HAM 4 (dated to 11.44 Ma) and HAM 5 (dated to 11.62 Ma), have been intensively excavated since 2011. The HAM 4 channel represents a larger meandering stream of about 50 m width, whereas the structure HAM 5 is interpreted as a meandering rivulet of 4–5 m width (Kirscher et al. 2016; Lechner and Böhme 2022).

In addition to these main fossiliferous horizons, a third vertebrate-bearing level (HAM 6) has been discovered and sampled by private collectors (Sigulf Guggenmos, Dösingen and Manfred Schmid, Marktoberdorf) during the late 1970s and early 1980s (Fig. 3). This horizon, which contained a partial proboscidean skeleton, was found directly below the upper lignite seam at the uppermost limit of the Miocene succession exposed in the clay-pit (see below), which imply, according to the age-model (Kirscher et al. 2016), an age of about 11.42 Ma for the site HAM 6.

These three fossil-bearing horizons, but especially the actively excavated HAM 4 and HAM 5, are decidedly productive, resulting in a high diversity and disparity of vertebrates, including so far 146 species from 75 families. Most spectacular was the discovery of associated skeletons of the partially bipedal hominid *Danuvius guggenmosi* (Böhme et al. 2019, 2020) in HAM 5. So far, only a fraction of the enormous vertebrate fauna has been studied in detail, including carnivorans (Kargopoulos et al. 2021a, b, c, 2022), ruminants (Fuss et al. 2015; Hartung et al. 2020; Hartung and Böhme 2022), beavers (Lechner and Böhme 2022, 2023), small mammals (Mayr and Fahlbusch 1975; Prieto and Rummel 2009; Prieto et al. 2011; Prieto 2012; Prieto and Dam 2012) and birds (Mayr et al. 2020a, b, 2022).

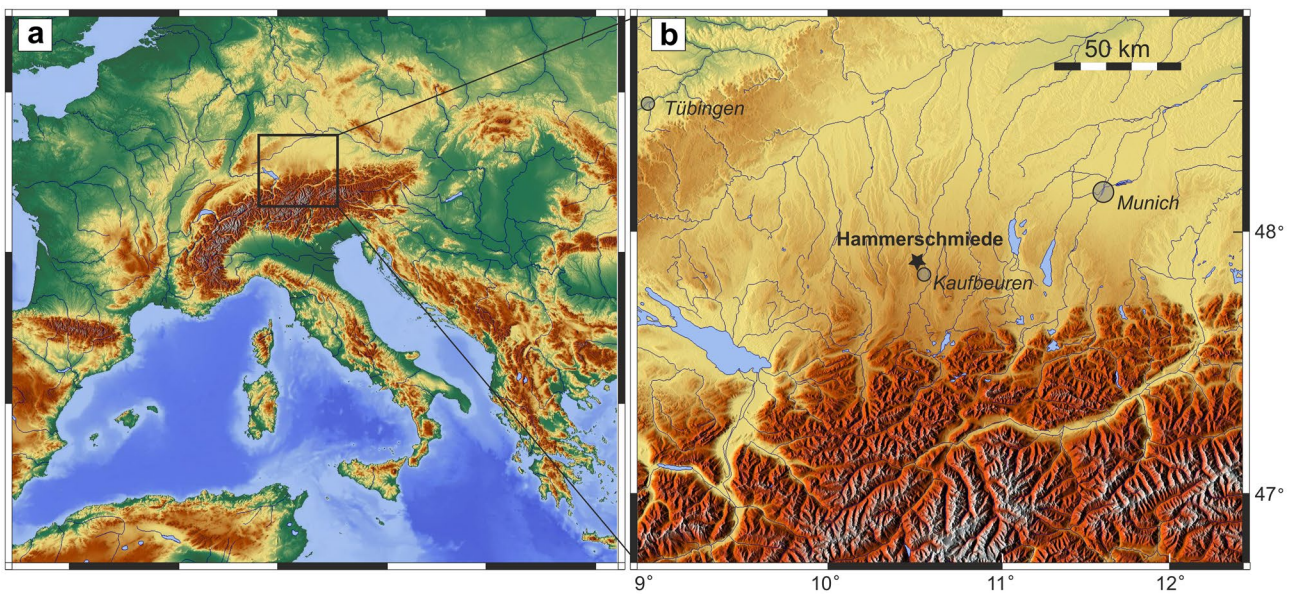

Fig. 1 Geographic position of the Hammerschmiede locality (Bavaria, Germany) in Europe (**a**) and in the North Alpine Foreland Basin (**b**)

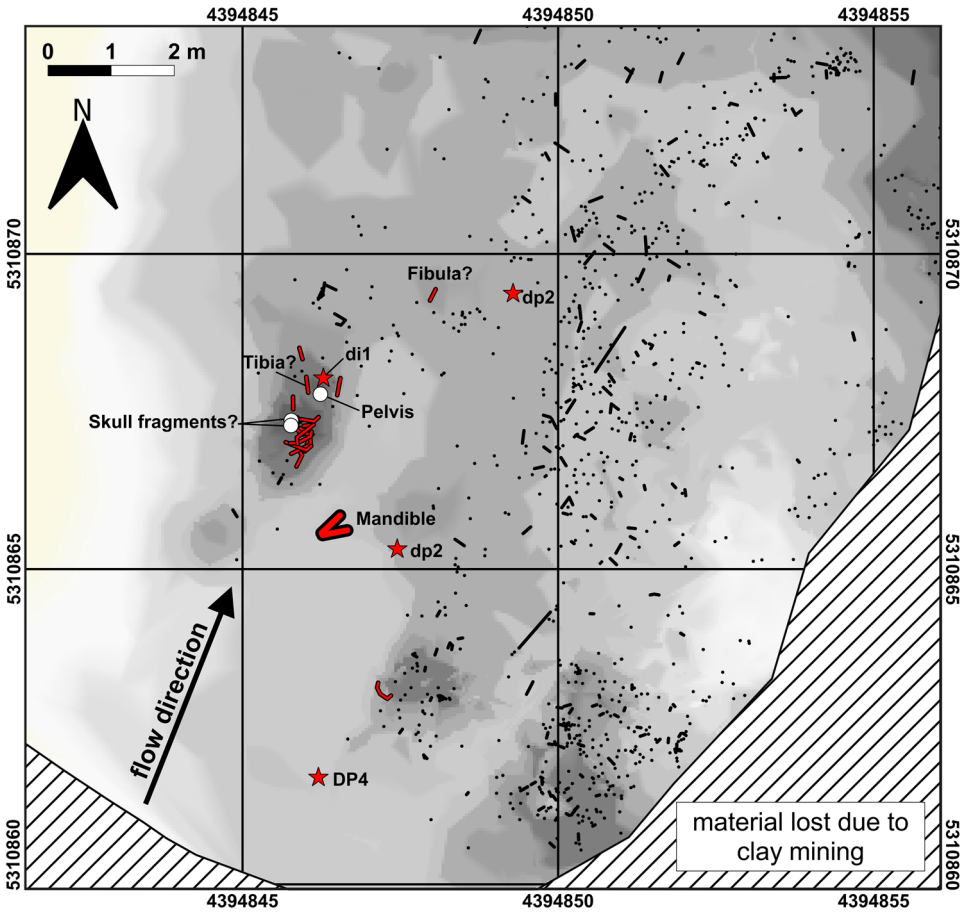

Fig. 2 Section of the excavation plan at Hammerschmiede HAM 5 (excavation years 2018–2021). Black dots represent vertebrate fossil specimens, black stripes denote elongated objects and their orientation. Excavated deinothere bones, most probably belonging to the same juvenile individual of *Deinotherium levius*, are highlighted with red stars (single teeth), a thick red angled line (mandible), white circles (pelvis and two skull fragments) and red lines (14 ribs, one tibia? and fibula?). Associated bones of the juvenile *Deinotherium* individual are arranged over a distance of eight meters parallel to the reconstructed flow direction in a shallower side branch of the HAM 5 rivulet. The background color indicates the elevation differences of the excavated palaeo-channel base, dark areas represent lower and brighter ones for higher elevations of the riverbed with a total height difference of 1.5 m, with finds only in the lowermost 70 cm. Note the uneven channel base and accumulation of most of the finds in pit-like depressions, which probably acted as bone traps. Coordinates correspond to Gauss-Krüger Zone 4 grid in meters

Material and methods

The herein studied proboscidean material originates from the layers HAM 4, HAM 5 and HAM 6 of the Hammerschmiede clay pit. All specimens are stored at the Palaeontological Collection of the University of Tübingen, Germany (GPIT), and are labelled as either GPIT/MA (for excavation years 2011–2019) or SNSB-BSPG (for excavation years 2020–2021). SNSB-BSPG-2020-XCIV refers to specimens from HAM 4 and SNSB-BSPG-2020-XCV from HAM 5. Comparative material was studied at FSL, HGI, HLMD, HNHM, ML, MNHN, NHMW, SNSB-BSPG and SU. The deinothere dental terminology follows Pickford and Pourabrishami (2013), and the gomphothere one is according to Tassy (1996a). For the cheek teeth, the metric parameters measured are the mesiodistal crown length (L), the maximum buccolingual crown width (W) in each loph(id), and the maximum height for unworn (or minimally worn) teeth. For the lower tusk of *Tetralophodon*, the compression index (Ci) was calculated as height × 100 / width. The measurements were taken with a digital caliper or, in the case of some large mandibular measurements, with a measuring tape; those in parentheses indicate the greatest measurable value of a parameter in incomplete or inadequately preserved specimens. Mandibular measurements follow Tassy (1996b). All measurements are given in Tables 1 and 2. Comparative dental measurements were obtained from the literature or directly acquired from specimens at several museums and institutions (Tables 3 and 4). For each deciduous tooth measurement and deinothere species used in the analysis,

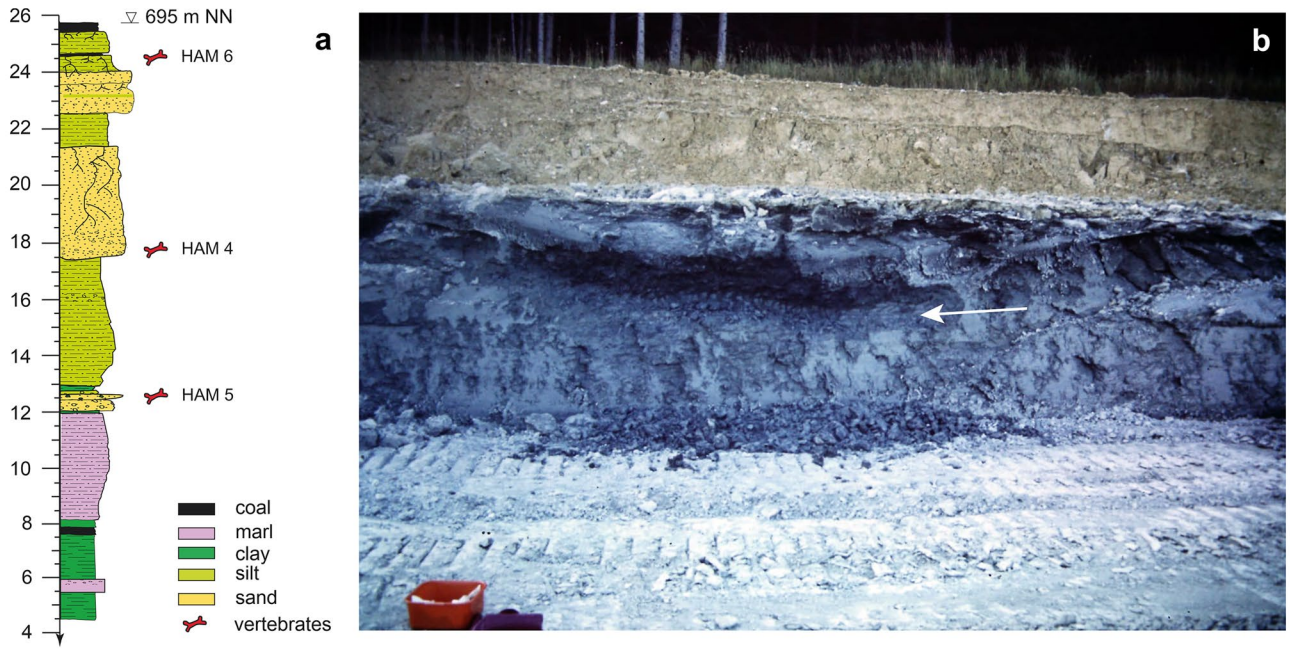

Fig. 3 **a.** Stratigraphic sequence (left) of the Hammerschmiede claypit (northern profile of Kirscher et al. 2016) indicating all three fossiliferous levels containing proboscideans. **b.** Finding position of the adult *Tetralophodon* skeleton (photo: M. Schmid, 1980). The Miocene clay-rich sediments are greyish-bluish in color and overlaid by bright-yellowish meltwater deposits of the Günz glaciation (earliest Middle Pleistocene). The excavated layer (HAM 6) is marked by the white arrow

the z-score was computed as $z = (x - m) / SD$, where x is the dental measurement of the HAM specimens (mean value in case both right and left deciduous premolar are preserved), and m and SD the mean and standard deviation of the comparative sample, respectively (Table 5).

Table 1 Mandibular measurements (in mm) of the *Deinotherium levius* mandible from Hammerschmiede 5

	Deinotherium levius
Mandibular measurements	SNSB-BSPG-2020-XCV-0096
preserved length	435
symphyseal length	91
alveolar distance	220
maximal width	277
mandibular width at the root of the rami	239
width of corpus at the root of the ramus	(75)
width of corpus infront of the dp2 alveolus	47
posterior symphyseal width	125
anterior symphyseal width	95
maximal width of the rostral trough	51
minimal width of the rostral trough	28
internal width between the dp2 alveoli	43
maximal height of corpus	(57)
rostral height at the symphyseal border	52
maximal depth of the ramus	139

In order to estimate the age at death of the *Tetralophodon* individual(s) from HAM 6, we applied the dental-wear-based criteria proposed by Metz-Muller (2000) for the tetralophodont gomphothere *Anancus arvernensis* (note, however, that *A. arvernensis* did not possess premolars and is thus not precisely comparable). Wear was codified as f, p, d, D and C (Metz-Muller 2000: figs. 20 and 21) for each of the four or five loph(id)s, and when necessary, separated between pretrite/posttrite lophids. Age estimation was based on the extant African elephant *Loxodonta africana* (Haynes 1991; Metz-Muller 2000: fig. 22) and thus the results should be considered indicative.

The deinothere mandible SNSB-BSPG-2020-XCV-0096 was scanned with an X-ray tube containing a multi-metal reflection target with a maximum acceleration voltage of 225 kV in the Nikon X TH 320 µCT scanner of the 3D imaging lab of the University of Tübingen using a 0.1 mm copper filter with 3500 projections, 200 kV and 27 µA, with a voxel size of 0.006741 mm. 3D models of the mandible, as well as from the associated to it right and left dp2 can be viewed in Online Resources 1–3. 3D renderings of the mandible are given in Online Resource 4, Figs. S1–S6.

In order to decipher the dietary habits of the Hammerschmiede proboscideans, we performed dental mesowear angle analysis (Saarinen et al. 2015). This method was originally applied in proboscideans with lamellar structure on their cheek teeth, and was later employed also in bunodont (e.g., *Gomphotherium*, *Tetralophodon*), zygodont

Table 2 Dental measurements (in mm) of *Deinotherium levius* and *Tetralophodon longirostris* from Hammerschmiede. Measurements in parentheses indicate the greatest measurable value of a parameter in incomplete or inadequately preserved specimens, or worn cusps in case of height values. Values noted with an asterisk were acquired from the CT-scan. Abbreviations: **L**, mesiodistal crown length; **H**, preserved crown height and cusp measured; **W**, maximum buccolingual crown breadth (at first, second, third and fourth loph/id)

Species	Inventory number	Site	Tooth	Side	L	W	W1	W2	W3	W4	W5	H
Deinotherium levius	SNSB-BSPG-2020-XCV-0199	HAM-5	dp2	right	31.4		18.3	20.1				29.3 (protoconid)
	SNSB-BSPG-2020-XCV-0092	HAM-5		left	30.7		17.4	19.9				27.6 (protoconid)
	SNSB-BSPG-2020-XCV-0257	HAM-5	di1	right	28.1	18.4						12.4
	SNSB-BSPG-2020-XCV-0096	HAM-5	dp3	right	(46.8)		-	37.0				29.0 (protoconid)
	SNSB-BSPG-2020-XCV-0096	HAM-5		left	52.2		31.1	35.4				-
	SNSB-BSPG-2020-XCV-0096	HAM-5	dp4	right	70.4			41.4*				-
	SNSB-BSPG-2020-XCV-0096	HAM-5		left	70.0			41.5				30.0 (3rd labial)
	SNSB-BSPG-2020-XCV-0096	HAM-5	i2	right	34.1*	27.8*						12.8*
	SNSB-BSPG-2020-XCV-0096	HAM-5	i2	left	37.5*	30.5*						-
	GPIT/MA/16490	HAM-4	DP2	right	36.9		28.8	32.1				28.3 (paracone)
	GPIT/MA/09552	HAM-5	DP3	left	47.8		42.8	47.0				(24.8) (paracone)
	GPIT/MA/13794	HAM-5	DP4	right	70.2		52.7	53.9	50.3			32.4 (protocone)
Tetralophodon longirostris	GPIT/MA/12313	HAM-5	dp4	right	78.6		36.6	38.9	42.4	35.4		-
	GPIT/MA/12196	HAM-5	DP3	left	51.1		32.5	41.8	39.7			(23.8) (metacone)
	GPIT/MA/09554	HAM-5	P3	right	(39.6)		41.1					
	GPIT/MA/10800–05	HAM-6	M1		(116)		(72)					
	GPIT/MA/10800–03	HAM-6	m2	right	143.3		64.0	71.5	80.1	65.8		(45.9) (3rd posttrite)
	GPIT/MA/10800–04	HAM-6	M2	left	144.0		85.9	83.0	85.0	79.1		(51.9) (3rd posttrite)
	GPIT/MA/10800–02	HAM-6	M3	right	191.2		97.3	96.3	94.1	92.4	77.3	49.6 (4th pretrite)

Table 3 Comparative sample of deinotheriid deciduous teeth used in the analyses

Taxon	Locality	Country	Age/MN	Source
Prodeinotherium cuvieri	Langenau 1	Germany	MN 4	Sach and Heizmann (2001)
	Chevilly	France	MN 4	Ginsburg and Chevrier (2001)
	Montreal-du-Gers	France	MN 4	Ginsburg and Chevrier (2001)
	ZagyvapalfaIva	Hungary	MN 4	Gasparik (2004)
Prodeinotherium bavaricum	Grund	Austria	MN 5	G.K. at NHMW
	Gračanica	Bosnia-Herzegovina	late MN 5 or early MN 6	Göhlich (2020)
	Channay-sur-Lathan	France	MN 5	Ginsburg and Chevrier (2001)
	Hommes	France	MN 5	Ginsburg and Chevrier (2001)
	Noyant	France	MN 5	Ginsburg and Chevrier (2001)
	Pont-Boutard	France	MN 5	Ginsburg and Chevrier (2001)
	Pontlevoy	France	MN 5	Stehlin (1925); Ginsburg and Chevrier (2001)
	Savigne-sur-Lathan	France	MN 5	Ginsburg and Chevrier (2001)
	Tavers	France	MN 5	Ginsburg and Chevrier (2001)
Deinotherium levius or *D. ?levius*	Hollabrunn	Austria	?	Huttunen (2002b)
	Atzelsdorf	Austria	earliest MN 9	Göhlich and Huttunen (2009)
	Mannersdorf bei Leithagebirge	Austria	?	Huttunen (2002b)
	Vetren	Bulgaria	?	Vergiev and Markov (2012)
	La Grive	France	MN 7/8	Ginsburg and Chevrier (2001); G.K. at ML
	Emmering bei Fürstenfeldbruck	Germany	?	Stromer (1940)
	Massenhausen	Germany	MN 7/8	G.K. at SNSB-BSPG
	Sopron	Hungary	late MN 7/8	G.K. at HNHM
	Charmoile	Switzerland	MN 9	Gagliardi et al. (2021)
Deinotherium giganteum or *D. ?giganteum*	Nessebar	Bulgaria	late Miocene	G.K. at SU
	Montredon	France	MN 10	G.K. at FSL and ML
	Rudabanya	Hungary	MN 9	Gasparik (2005)
	Kayadibi	Turkey	late Miocene (?Vallesian)	Gaziry (1976)
D. proavum	Wolfau	Austria	Pannonian	G.K. at NHMW
	Rogozen	Bulgaria	late Miocene	G.K. at SU
	Pikermi	Greece	MN 12	Wagner (1848, 1857); Konidaris et al. (2017)
	Samos	Greece	Turolian	Konidaris and Koufos (2019)
	Baltavar	Hungary	MN 12	Gasparik (2004); G.K. at HNHM
	Pestszentlörinc	Hungary	Turolian	Gasparik (2004)
	Polgardi	Hungary	MN 13	G.K. at HNHM
	Cimislia	Moldova	MN 12	Simionescu and Barbu (1939)
	Taraklia	Moldova	MN 12	Khomenko (1914)
	Kiro Kucuk	North Macedonia	Turolian	Garevski and Markov (2011)
	Sinap 49	Turkey	late MN 10	Sanders (2003)

(e.g., *Mammut*) and lophodont (deinotheres) proboscideans (Saarinen and Lister 2016; Xafis et al. 2020). Here we apply the method only in *Tetralophodon* molars, because the HAM deinothere teeth are deciduous, they are almost unworn and do not have sufficiently worn facets. Angles were measured from the bottom (deepest point) of the dentine valleys in moderately worn main cusps to the top of the cusp's enamel ridges. For this purpose, we used a contour gauge that we have precisely fit within the cusp where the angle was to be measured. The contour gauge was photographed

Table 4 Comparative sample of tetralophodont molars used in the analyses ("Dinotheriensande" sites are noted with D)

Taxon	Locality	Country	Age/MN	Source
Tetralophodon longirostris	Atzelsdorf	Austria	earliest MN 9	Göhlich and Huttunen (2009)
	Auersbach	Austria	Vallesian	Göhlich (1998)
	Belvedere	Austria	Vallesian	Göhlich (1998); G.K. at NHMW
	Breitenfeld	Austria	MN 9	Göhlich (1998)
	Eggersdorf	Austria	Vallesian	Göhlich (1998)
	Geiereck	Austria	?	Göhlich (1998)
	Gschmeier	Austria	Vallesian	Göhlich (1998)
	Kornberg	Austria	MN 9	Göhlich (1998)
	Laaerberg	Austria	MN 9	Schlesinger (1917)
	Lasnitz	Austria	Vallesian	Göhlich (1998)
	Laßnitzhöhle	Austria	?	Göhlich (1998)
	Mannersdorf	Austria	?	Göhlich (1998); G.K. at NHMW
	Meidling	Austria	Vallesian	Göhlich (1998)
	Obertiefenbach	Austria	Vallesian	Göhlich (1998)
	Stettenhof	Austria	Vallesian	Göhlich (1998)
	Wolfau	Austria	Vallesian	Göhlich (1998)
	Dinotheriensande (D)	Germany	middle–late Miocene	Göhlich (1998)
	Bermersheim (D)	Germany	middle–late Miocene	Göhlich (1998); G.K. at HLMD
	Eppelsheim (D)	Germany	middle–late Miocene	Klähn (1931); Göhlich (1998); Gaziry (1994); G.K. at HLMD and MNHN
	Esselborn (D)	Germany	middle–late Miocene	Bergounioux and Crouzel (1960); Göhlich (1998)
	Gegend Alzey (D)	Germany	middle–late Miocene	Göhlich (1998)
	Kahlig bei Bermersheim (D)	Germany	middle–late Miocene	Göhlich (1998)
	Westhofen (D)	Germany	middle–late Miocene	Gaziry (1994)
	Wissberg (D)	Germany	middle–late Miocene	Göhlich (1998)
	Rudabanya	Hungary	MN 9	Gasparik (2004, 2005); G.K. at HGI
	Azambujeira (middle level)	Portugal	Vallesian	Antunes and Mazo (1983)
	Kapellen	Slovenia	Vallesian	Göhlich (1998)
	Polinya	Spain	MN 9	Alberdi (1971)
Konobelodon atticus or *Konobelodon* sp.	Maritsa-Iztok	Bulgaria	Turolian	Kovachev (2004)
	Oryahovo	Bulgaria	late Miocene	G.K. at SU
	Pestszentlörinc	Hungary	Turolian	G.K. at HNHM
	Yulafli	Turkey	MN 10	Geraads et al. (2005)
?*Stegotetrabelodon*	Crevilente 2	Spain	MN 11	Mazo and Montoya (2003)
tetralophodont indet.	Mannersdorf bei Angern	Austria	Panonian F/H	G.K. at NHMW
	Küçükcekmece	Turkey	MN 10	Tassy (2016)

Table 5 Descriptive statistics and calculated z-scores for the dental measurements (in mm) of the HAM deinotheriid deciduous teeth compared to *Prodeinotherium cuvieri, Prodeinotherium bavaricum, Deinotherium levius, Deinotherium giganteum and Deinotherium proavum* from several localities (see Materials and methods, and Table 3). When z >|1.96|, the null hypothesis that the HAM specimens fit within the variation of the comparative sample can be rejected at $p < 0.05$; in such cases the z-score is typed in bold). Abbreviations: **CI,** confidence interval; **L,** mesio-distal crown length; ***n*,** number of specimens; **W,** maximum buccolingual crown breadth; **SD,** standard deviation

		n	mean	minimum	maximum	SD	95% CI (lower)	95% CI (upper)	z-score
LDP2	HAM	1	36.90						
	P. cuvieri	1	28.30	-	-	-	-	-	
	P. bavaricum	3	26.33	24.8	29.0	2.32	20.58	32.09	**4.56**
	D. levius	4	36.25	35.0	39.0	1.86	33.28	39.22	0.35
	D. giganteum	5	41.26	36.4	44.0	2.93	37.63	44.89	-1.49
	D. proavum	7	48.57	40.6	53.9	4.49	44.42	52.72	**-2.60**
WDP2	HAM	1	32.10						
	P. cuvieri	1	24.30	-	-	-	-	-	
	P. bavaricum	3	22.83	19.7	27.0	3.76	13.50	32.17	**2.47**
	D. levius	4	30.93	29.5	32.2	1.37	28.74	33.11	0.85
	D. giganteum	5	37.70	32.6	42.0	3.60	33.23	42.17	-1.56
	D. proavum	7	45.03	41.9	47.1	2.04	43.15	46.91	**-6.34**
LDP3	HAM	1	47.80						
	P. cuvieri	3	33.47	32.1	34.4	1.21	30.46	36.47	**11.84**
	P. bavaricum	5	35.72	33.0	38.0	1.92	33.34	38.10	**6.29**
	D. levius	4	44.58	42.0	48.0	2.92	39.93	49.22	1.10
	D. giganteum	2	52.65	51.3	54.0	1.91	35.50	69.80	**-2.54**
	D. proavum	12	58.39	48.0	64.2	4.51	55.52	61.26	**-2.35**
WDP3	HAM	1	47.00						
	P. cuvieri	3	27.83	24.0	31.0	3.55	19.02	36.65	**5.40**
	P. bavaricum	5	31.96	29.0	34.0	2.39	28.99	34.93	**6.29**
	D. levius	4	40.23	38.6	42.3	1.74	37.46	42.99	**3.89**
	D. giganteum	2	50.00	50.0	50.0	0	-	-	-
	D. proavum	12	57.47	52.4	64.7	3.24	55.41	59.53	**-3.23**
LDP4	HAM	1	70.20						
	P. cuvieri	2	55.05	55.0	55.1	0.07	54.41	55.69	**216.43**
	P. bavaricum	9	53.84	49.0	60.8	3.97	50.80	56.89	**4.12**
	D. levius	4	67.23	64.2	71.8	3.26	62.04	72.41	0.91
	D. giganteum	3	75.47	70.4	78.0	4.39	64.57	86.37	-1.20
	D. proavum	5	86.82	82.9	91.2	3.58	82.37	91.27	**-4.64**
WDP4	HAM	1	53.90						
	P. cuvieri	2	37.90	37.8	38.0	0.14	36.63	39.17	**114.29**
	P. bavaricum	9	38.33	34.0	40.8	2.53	36.39	40.28	**6.15**

Table 5 (continued)

		n	mean	minimum	maximum	SD	95% CI (lower)	95% CI (upper)	z-score
	D. levius	4	50.75	48.5	54.7	2.86	46.20	55.30	1.10
	D. giganteum	3	56.33	52.0	59.0	3.79	46.93	65.74	-0.64
	D. proavum	5	67.42	63.0	69.0	2.50	64.32	70.52	**-5.41**
Ldp2	HAM	2	31.05	30.7	31.4	0.49			
	P. cuvieri	1	19.00	-	-	-	-	-	-
	P. bavaricum	3	20.93	17.5	23.3	3.04	13.37	28.49	**3.33**
	D. levius	4	27.70	26.4	28.9	1.24	25.73	29.67	**2.70**
	D. giganteum	5	31.50	29.9	33.5	1.66	29.44	33.56	-0.27
	D. proavum	3	34.37	33.8	35.4	0.90	32.14	36.59	**-3.69**
Wdp2	HAM	2	20.00	19.9	20.1	0.14			
	P. cuvieri	1	11.50	-	-	-	-	-	-
	P. bavaricum	3	14.87	11.0	17.2	3.37	6.49	23.24	1.52
	D. levius	4	18.65	16.8	20.0	1.45	16.34	20.97	0.93
	D. giganteum	5	22.82	21.0	25.0	1.66	20.76	24.88	-1.70
	D. proavum	3	27.83	23.2	30.2	4.01	17.87	37.80	-1.95
Ldp3	HAM	1	52.20						
	P. bavaricum	8	36.23	34.0	38.5	1.60	34.89	37.56	**9.98**
	D. levius	3	45.90	45.7	46.2	0.26	45.24	46.56	**24.23**
	D. giganteum	6	54.20	51.1	56.0	1.76	52.37	56.06	-1.14
	D. proavum	6	60.60	54.6	64.1	3.75	56.63	64.50	**-2.24**
Wdp3	HAM	1	35.40						
	P. bavaricum	8	25.01	20.0	29.9	3.31	22.25	27.78	**3.14**
	D. levius	3	31.37	30.8	31.7	0.49	30.14	32.59	**8.22**
	D. giganteum	6	37.40	34.5	40.1	1.86	35.45	39.35	-1.08
	D. proavum	6	42.55	37.3	44.8	2.77	39.65	45.46	**-2.58**
Ldp4	HAM	2	70.20	70.0	70.4	0.28			
	P. bavaricum	10	50.94	39.5	58.1	1.54	47.45	54.43	**12.51**
	D. levius	6	66.25	57.7	69.7	4.40	61.63	70.87	0.90
	D. giganteum	7	77.73	71.0	82.0	3.74	74.27	81.19	**-2.01**
	D. proavum	5	86.30	79.5	90.3	4.28	80.98	91.62	**-3.76**
Wdp4	HAM	2	41.45				41.40	41.50	
	P. bavaricum	10	29.50	1.90	28.1	30.9	26.5	32.8	**6.29**
	D. levius	6	39.43	2.63	36.7	42.2	37	44.3	0.77
	D. giganteum	8	46.06	2.95	43.6	48.5	42.6	50	-1.56
	D. proavum	5	52.54	6.13	44.9	60.2	42.6	58	-1.81

Table 6 Dental mesowear angles of the *Tetralophodon longirostris* sample from Hammerschmiede 6 and summary statistics. Abbreviations as in Table 5

Tooth	Inventory number	Cusp measured	Mesowear angle (°)	Mean mesowear angle (°)
m2	GPIT/MA/10800–03	2 pretrite	117.6	117.1
		2 posttrite	116.5	
M2	GPIT/MA/10800–04	2 pretrite	116.7	116.7
M3	GPIT/MA/10800–02	3 posttrite	105.3	104.3
		3 pretrite	103.3	
Mean				112.7
Median				116.7
SD				7.28
95% CI (lower)				94.6
95% CI (upper)				130.8

horizontally from a vertical position and was subsequently processed in ImageJ (Abràmoff et al. 2004; https://imagej.nih.gov/ij/index.html), where the angle was measured from the relief formed at the upper (counter) side of the contour gauge (see Saarinen et al. 2015: fig. 1b). This process was applied in all measurable cusps of each tooth (pretrite and/or posttrite sides) and the mean value was calculated for each tooth (Table 6). The mesowear angles from HAM were compared with the dataset of Xafis et al. (2020), which includes mesowear angles for Miocene proboscideans of Eurasia.

Box-and-whisker plots and statistical computations were performed with PAST v. 4.12 (Hammer et al. 2001; https://www.nhm.uio.no/english/research/resources/past/).

Institutional abbreviations: FSL, Faculté des Sciences de Lyon (France); **HGI**, Hungarian Geological Institute (Budapest); **HLMD**, Hessisches Landesmuseum Darmstadt (Germany); **HNHM**, Hungarian National History Museum, Budapest (Hungary); **ML**, Musée des Confluences, Lyon (France); **MNHN**, Muséum National d'Histoire Naturelle (Paris, France); **NHMW**, Naturhistorisches Museum Wien (Austria); **SNSB-BSPG**, Staatliche Naturwissenschaftliche Sammlungen Bayerns—Bayerische Staatssammlung für Paläontologie und Geologie, München (Germany); **SU**, Palaeontology Museum of Sofia University (Bulgaria).

Dental abbreviations: **aprcc1, 2, 3**, anterior pretrite central conule of the first, second or third loph(id); **di**, lower deciduous tusk; **dp/DP**, lower/upper deciduous premolar; **m/M**, lower/upper molar; **ppocc1, 2**, posterior posttrite central conule of the first or second loph (id); **pprcc1, 2, 3**, posterior pretrite central conule of the first, second or third loph(id).

Taphonomic remarks on the partial skeletons from HAM 5 and HAM 6

Deinotherium at HAM 5: In total 24 bones and isolated teeth of a juvenile *Deinotherium* from the overbank extension of the HAM 5 rivulet belong to the same individual. The proposed strewnfield consists of a mandible, right DP4, left and right dp2, di1, two cranial fragments of unknown position, possibly the tibia and the fibula, the pubis and 14 ribs. These specimens were excavated during the field seasons in 2018, 2020 and 2021 over a distance of eight meters parallel to the reconstructed flow direction (SSW–NNE) of the rivulet (Fig. 2). The arrangement of the bones corresponds approximately to the typical sorting by density and bone volume (Voorhies 1969; Behrensmeyer 1975), with the heavier and denser DP4 and mandible in the southernmost limit of the strewnfield and the lighter and less dense bones north of it. A special feature is the accumulation of a large proportion of the finds (especially ribs) in a pit-like erosion depression on the more lithified bedrock. This depression in the channel base probably acted as a bone trap through the resulting flow shadow. The proximate spatial accumulation of the deinothere remains, the absence of duplicate skeletal elements, the consistency in ontogenetic age of both dental and postcranial remains, as well as in dental wear, combined with the fact that all of the surrounding finds belong to other taxa, indicate that the *Deinotherium* remains were deposited in a single taphonomic event and represent a single individual.

Tetralophodon at HAM 6: A partial adult skeleton has been independently excavated by the two private collectors Sigulf Guggenmoos (Dösingen) in the end of 1970ies and Manfred Schmid (Marktoberdorf) in early 1980ies. The finding position of the material was at the uppermost part of the Miocene sediments exposed at the time in the Hammerschmiede clay-pit, below the presently exposed upper lignite seam (Fig. 3). Both collections contain, besides upper and lower tusks and molars, hundreds of heavily fractured bone fragments. This fragmentation, which prohibits morphological and taphonomic investigations, is probably related to the heavy machinery removing the directly overlying till (Fig. 3) of Middle Pleistocene

age (Riss glaciation) or was caused by Pleistocene glacial processes. While the tooth collections show no duplicates, however, and although there is consistency in dental wear between the m2 and M2, the substantially more worn M3 than M2 (see below) is not compatible with the dental succession and normal wear pattern known in elephantimorph proboscideans indicating the presence of either two individuals, or one with anomalous/pathologic condition.

Systematic palaeontology

Mammalia Linnaeus, 1758
Proboscidea Illiger, 1811
Deinotherioidea Osborn, 1921
Deinotheriidae Bonaparte, 1845
Deinotherium Kaup, 1829
Deinotherium levius Jourdan, 1861

Type material: ML-LGR-962 (lectotype), right upper toothrow with P3–M3; figured in Depéret (1887: pl. 18, fig. 1).

Type locality: La Grive Saint-Alban, quarry Peyre et Beau, France, Middle Miocene (MN 8).

Material (HAM 4): right DP2, GPIT/MA/16490.

Material (HAM 5): partial juvenile skeleton (see Fig. 2), represented by 24 specimens including the mandible with erupting right and left lower tusks and right and left dp3–dp4, SNSB-BSPG-2020-XCV-0096; right di1, SNSB-BSPG-2020-XCV-0257; right dp2, SNSB-BSPG-2020-XCV-0199; left dp2, SNSB-BSPG-2020-XCV-0092; right DP4, GPIT/MA/13794, two cranial fragments of unknown position, SNSB-BSPG-2020-XCV-0253–11 and 0253–12, as well as the pubis SNSB-BSPG-2020-XCV-0256; ?fibula, SNSB-BSPG-2020-XCV-0358); ?tibia, SNSB-BSPG-2020-XCV-0433; and 14 ribs GPIT/MA/13773, SNSB-BSPG-2020-XCV-0252, 0253–01, 0253–02, 0253–03, 0253–04, 0253–05, 0253–06, 0253–07, 0253–08, 0253–09 and 0253–10. In addition to this partial skeleton, this horizon yields a left DP3, GPIT/MA/09552, and multiple worn and unworn molar fragments (GPIT/MA/09553, 09867, 10,338, 10,340).

Description

Mandible and lower dentition The mandible is almost complete, preserving the corpora with the symphysis and the rami with their coronoid processes; both hemimandibles lack the region of the mandibular angle and have partially damaged condyles (Fig. 4; Online Resources 1 and 4: Figs. S1–S6). The mandible bears the right and left dp3 and dp4, while the alveoli of the dp2 are open (Fig. 4a); these alveoli most possibly fit the isolated right and left dp2s (described below), which were found in spatial proximity with the mandible and are compatible in terms of wear stage with the other deciduous dentition. Additionally, two emerging lower tusks are visible inside their alveoli within the symphysis; they are postdepositionally compressed dorsoventally. They are covered with enamel, but there is no distinct cervix, and the pulp cavity is open (Figs. 4d, f and 5); as such the tusks are identified as permanent (juvenile) lower tusks (i2). The enamel is thick at their tips and becomes thinner distally. The symphysis is ventrally deflected. Two foramina are present, one large at the level of the caudal symphyseal border, and one smaller at the level of the distal part of the dp2 alveolus. Both rostral and caudal margins of the ramus are caudally inclined relative to the corpus.

The lower deciduous tusk SNSB-BSPG-2020-XCV-0257 is complete (total length: 100 mm) and strongly curved (Fig. 6j–m). Its tip is covered by a short enamel cap, which is well separated by a distinct cervix from the root. The maximum diameters of the root (21.1 × 13.4 mm) are almost at its middle, while it narrows towards the proximal part. The pulp cavity is closed.

Both left and right dp2s (SNSB-BSPG-2020-XCV-0092 and 0199) are almost unworn apart from the worn ectolophid and hypoconid (Fig. 6n–s; Online Resources 2 and 3). They most probably both belong to the same individual as the mandible SNSB-BSPG 2020-XCV-0096. They have a triangular shape with narrow and high mesial part, and two fused roots. The paracristid consists of several weak conelets decreasing in height, but there is one strong one in front of the protoconid. The protoconid, which is set in a more mesiolabial position than the metaconid, is separated from the latter and there are two conelets in between them. The ectolophid connects the protoconid with the hypoconid. The hypoconid and entoconid are opposite to each other and are connected with a series of weak conelets positioned in line and decreasing in size from the former to the latter cusp; hypoconid is higher than entoconid. The distal cingulum is low and is comprised by several weak conelets in a row.

The right dp3 is slightly damaged, especially in its mesiolingual part, whereas the left one is well-preserved (Fig. 4; Online Resource 4). It is almost unworn, apart from the protoconid, which shows a worn facet at its tip, and the crests connecting the main cusps in each lophid. The tooth consists of two lophids, of which the mesial one is narrower. The strong and curved mesial cingulum, which is comprised by a series of cusplets, is connected through the preprotocristid (paracristid) with the protoconid. On the lingual side, the mesial cingulum extends until the prematacristid, which runs in front of the metaconid. One low

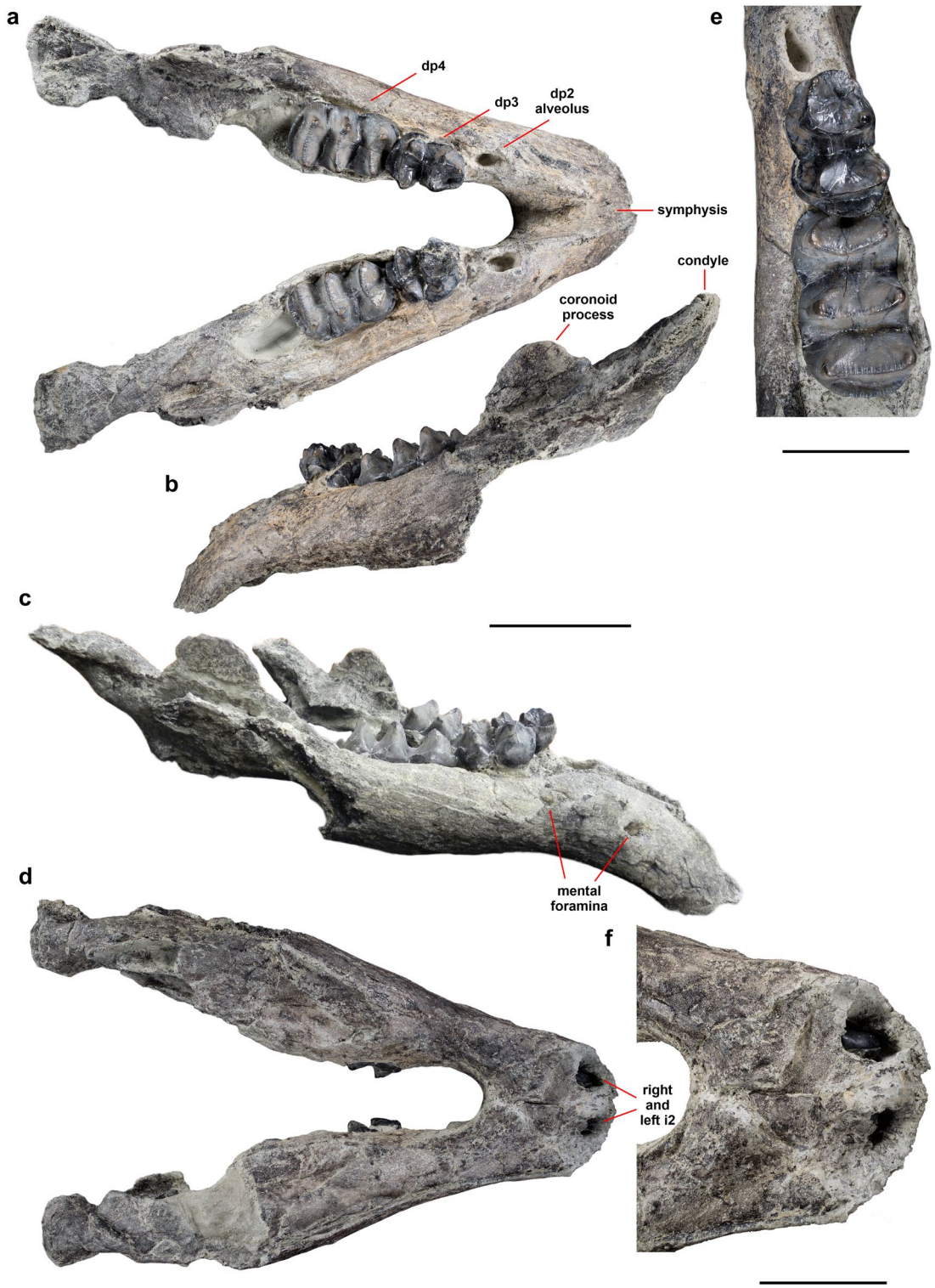

Fig. 4 Juvenile mandible (SNSB-BSPG-2020-XCV-0096) with erupting right and left i2, and right and left dp3–dp4 of *Deinotherium levius* from Hammerschmiede 5 in dorsal (**a**), left lateral (**b**), right lateral (**c**) and ventral (**d**) view; occlusal view of the left dp3 and dp4 (**e**); close-up view of the ventral side of the symphysis showing the emerging i2 (**f**). Scale bars equal 10 cm in a–d, and 5 cm in e–f

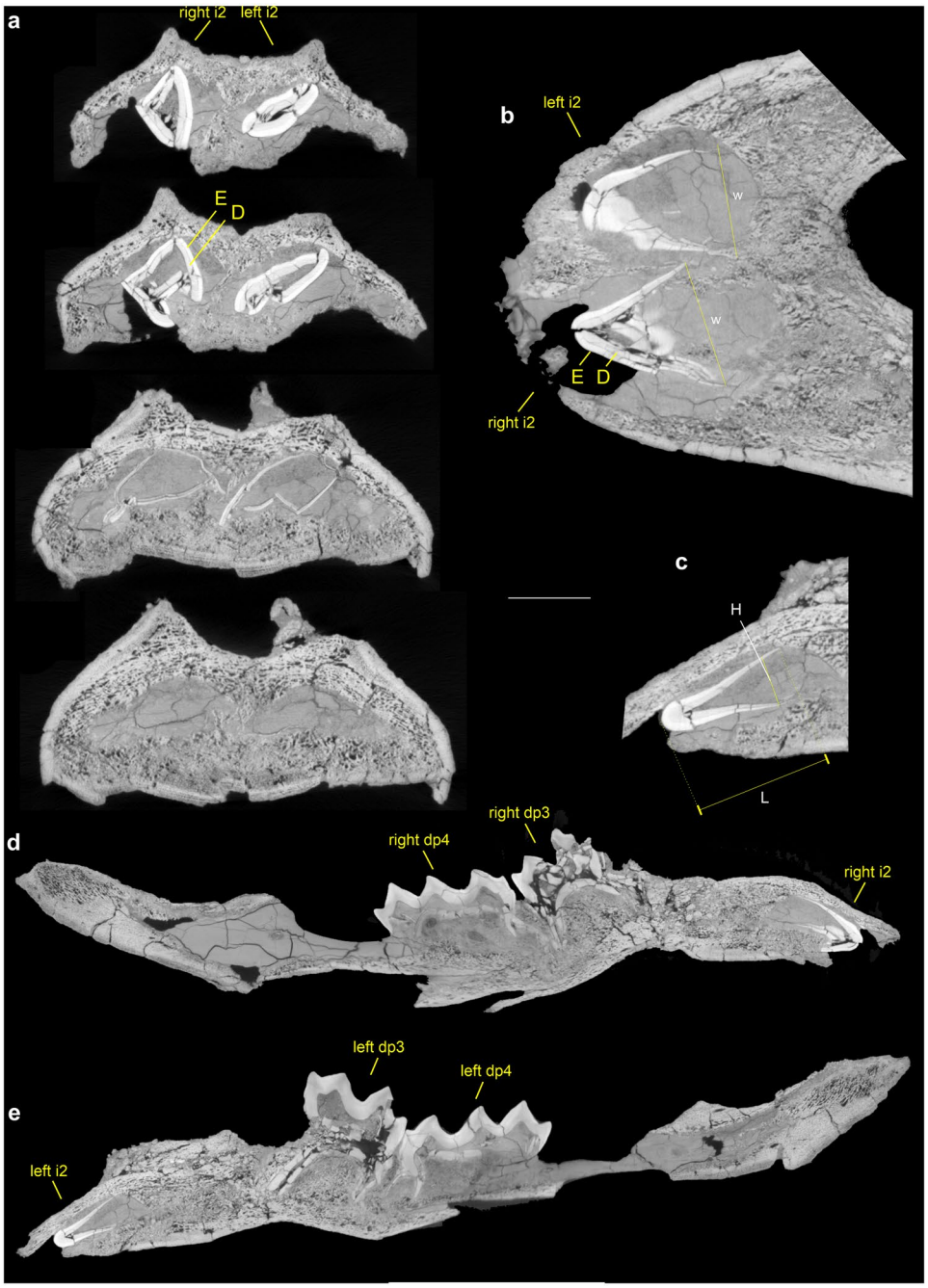

Fig. 5 CT-scan slices of the *Deinotherium levius* mandible (SNSB-BSPG-2020-XCV-0096) from Hammerschmiede 5. **a.** Coronal slices in the symphysis showing the right and left lower permanent tusks (i2) and their alveoli (from anterior to posterior from top to bottom). **b.** transverse slice in the symphysis showing the right and left i2; noted are the enamel (E) and the dentine (D) of the tusks, and the measured width (W). **c.** Parasagittal slice in the symphysis showing the right lower tusk, and the measured length (L) and height (H). **d.** Parasagittal slice of the right hemimandible. **e.** Parasagittal slice of the left hemimandible. Scale bars equal 20 mm in **a–c** and 100 mm in **d–e**. Additional CT-scan slices are given in Online Resource 4, Fig. S7

cusplet (rudimentary cingulum?) is located at the mesiolabial side of the tooth. The slightly worn and distally curved protolophid connects proto- and metaconid. The transverse valley is open. The hypolophid is only slightly curved and connects the hypo- and entoconid. The pre-entocristid and prehypocristid are strong. The distal cingulum is separated from the hypolophid; it is strong but low and formed by a series of conelets.

The dp4 is trilophodont (Fig. 4; Online Resource 4). It is erupting from the mandible and is unworn. The mesial cingulum is weak and low. The crest connecting in the mesial lophid the main cusps is curved; this crest in lophid 2 is less curved, whereas in distal one is straight. The mesial cristid of the main cusps are visible in all lophids; those in the labial side are stronger and even more the more mesial one. The transverse valleys are open, but there are remnants of cingulum in the labial side. The distal cingulum is low and consists of a series of conelets.

Two erupting tusks are partially visible within the symphysis of the mandible, but their morphology can be further observed in virtual cross-section of the µCT-scan of the mandible (Fig. 5). They are recognized as permanent ones

Fig. 6 Dental remains of *Deinotherium levius* from Hammerschmiede. **a–c.** Right DP2, HAM 4, GPIT/MA/16490 in occlusal (**a**), labial (**b**) and lingual (**c**) view. **d–f.** Left DP3, HAM 5, GPIT/MA/09552 in occlusal (**d**), labial (**e**) and lingual (**f**) view. **g–i.** Right DP4, HAM 5, GPIT/MA/13794 in occlusal (**g**), labial (**h**), lingual (**i**) view. **j–m.** Right di1, HAM 5, SNSB-BSPG-2020-XCV-0257 in dorsal (**j**), ventral (**k**), lateral (**l**) and medial (**m**) view. **n–p.** Right dp2, HAM 5, SNSB-BSPG-2020-XCV-0199 in occlusal (**n**), lingual (**o**) and labial (**p**) view. **q–s.** Left dp2, HAM 5, SNSB-BSPG-2020-XCV-0092 in occlusal (**q**), lingual (**r**) and labial (**s**) view. Scale bar equals 5 cm

due to the absence of an enamel cap with distinct cervix and the clearly open pulp cavity. Like the rest of the mandible, the tusks are dorsoventrally compressed postdepositionally, and the enamel and the dentine are in several places offset. Despite this deformation, the cross-section can be generally regarded as subcircular. The tusks are covered by a continuous enamel layer, which becomes thinner towards the proximal part. Some small enamel buds are visible at the tip.

Upper dentition The isolated DP2 is bilophodont and practically unworn (Fig. 6a–c). It has a mesial cingulum, stronger and more pointed at the mesiolabial side, consisting of several conelets, while on its lingual side there are five to six low conelets. A slightly worn curved crest in loph 1 connects the protocone with the metacone. The ectoloph, connecting the paracone with the metacone, is continuous. On the lingual side, the proto- and hypocone are well separated by an open valley. The hypocone, which is damaged at its tip, is ornamented with several weak conelets at its labial side. The distal cingulum is low and consists of a series of very weak conelets, increasing in height labially and connect with the metacone.

The DP3 consists of two lophs, both of which are much worn, and as a result confluent dentine is exposed on proto- and metaloph (Fig. 6d–f). The mesial cingulum is developed, and the stronger parastyle is connected to the weaker protostyle by a worn ridge. A worn weak ridge connects the parastyle and the paracone. The lophs are clearly separated by marked ecto- and entoflexus; the transverse valley is open lingually, but blocked labially. The postparacrista and postmetacrista are well developed, the latter connected to the metastyle. The distal cingulum is partially damaged; it is low and weaker on the labial side.

The DP4 is trilophodont (Fig. 6g–i). The mesial cingulum is rather low, almost half the height of loph 1, but the parastyle is strong and is connected with the paracone by a weak ridge. Slightly mesially curved crests (more curved in loph 3) consisting of numerous conelets connect the main cusps of each loph. Both ectoflexus are pronounced, especially the first one. The postparacrista and postmetacrista are strong. There is "double" distal cingulum; the distalmost one is longer but lower, consisting of a series of weak conelets.

Remarks

Based on several dental, cranial and postcranial features, European deinotheres are represented by the Early–Middle Miocene *Prodeinotherium* and the Middle–Late Miocene *Deinotherium* (e.g., Huttunen 2002a; Aiglstorfer et al. 2014a; Konidaris et al. 2017). Five species are considered valid here: *Prodeinotherium cuvieri* (Kaup, 1832a) from the early–middle Orleanian, *Prodeinotherium bavaricum* (von Meyer, 1831) from the late Orleanian–early Astaracian, *Deinotherium levius* Jourdan, 1861 from the late Astaracian, *Deinotherium giganteum* Kaup, 1829 from the Vallesian and *Deinotherium proavum* (Eichwald, 1831) (= *Deinotherium gigantissimum* Stefanescu, 1892) from the latest Vallesian–Turolian. In the absence of clear-cut evidence of coexistence between chronologically successive species, it is generally regarded that European deinothere species did not have overlapping chronostratigraphic ranges. Distinctive features among the species include: a) dental dimensions, b) traits of the mandible (shape of the symphysis and the mandibular angle), and c) morphology of the p3 and the dp2/DP2. Further details on the taxonomy of European deinotheres are given in Aiglstorfer et al. (2014a), Konidaris et al. (2017), Alba et al. (2020) and Konidaris and Tsoukala (2022).

Comparison

Dental morphology remained relatively conservative throughout the evolutionary history of deinotheres, however, dental dimensions increased progressively throughout the Miocene in the European species, and besides their taxonomic value, they most importantly have biochronologic significance. The metric comparison (bivariate, and box-and-whisker plots) of the deciduous dentition reveals that although some overlap in the size ranges between chronologically successive species for certain tooth positions, their interquartile ranges are mostly non-overlapping, while the average dimensions are larger in each chronologically succeeding species. Such a distinction among the species, allows the metric comparison of the available teeth from HAM. For all tooth positions, the crown dimensions of the HAM deciduous teeth (Figs. 7 and 8) are clearly distinguished from both *Prodeinotherium* (*P. cuvieri* and *P. bavaricum*) and *D. proavum*. Therefore, we focus the comparison on *D. levius* and *D. giganteum*. For all tooth positions, the HAM crown dimensions are greater than the L and W mean and median values of *D. levius*, and lower than the values of *D. giganteum* (Figs. 8 and 9). The LDP2 and WDP2 values from HAM are at the lowermost range or outside, respectively, of *D. giganteum*; LDP2 stands within the upper part of the interquartile range, and WDP2 at the upper quartile of *D. levius* (Fig. 8). The HAM DP2 is plotted close to the *D. levius* specimens from La Grive (France), Massenhausen (Germany), Atzelsdorf (Austria) and to the *D. levius*-sized DP2 from Emmering bei Fürstenfeldbruck (Germany), while it overlaps only with the DP2 of *D.* ?*giganteum* from Nessebar (Bulgaria) (Fig. 7). The LDP3 value from HAM is much below the lower range of *D. giganteum* and plots at the upper range of *D. levius* [the

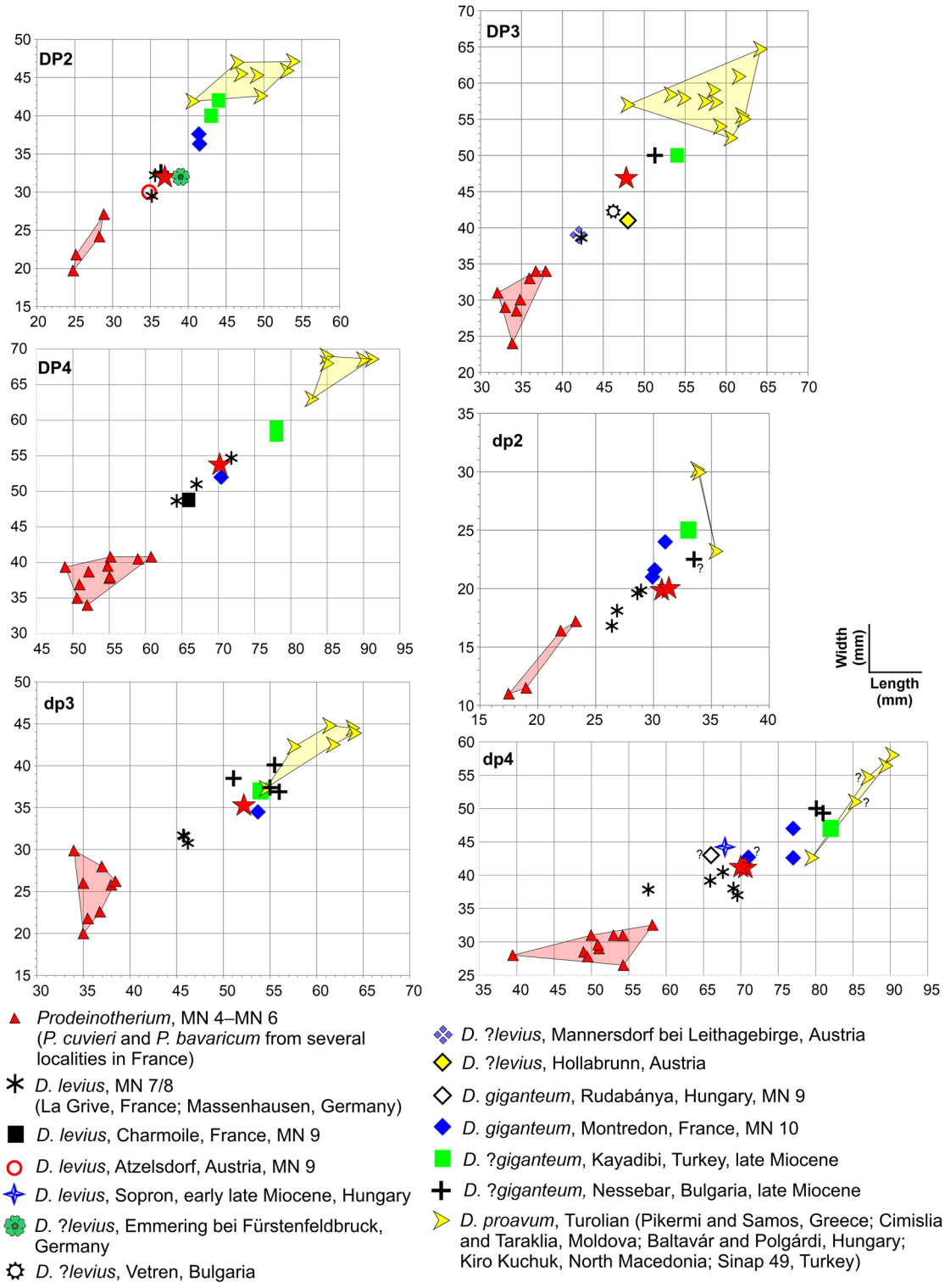

Fig. 7 Bivariate plots of length vs. maximum width (in mm) for deinotheriid lower and upper deciduous premolars from various localities. The symbol "?" indicates incomplete or inadequately preserved specimens; the convex hulls for *Prodeinotherium* and *Deinotherium proavum* are also shown. For the comparative sample, see Table 3

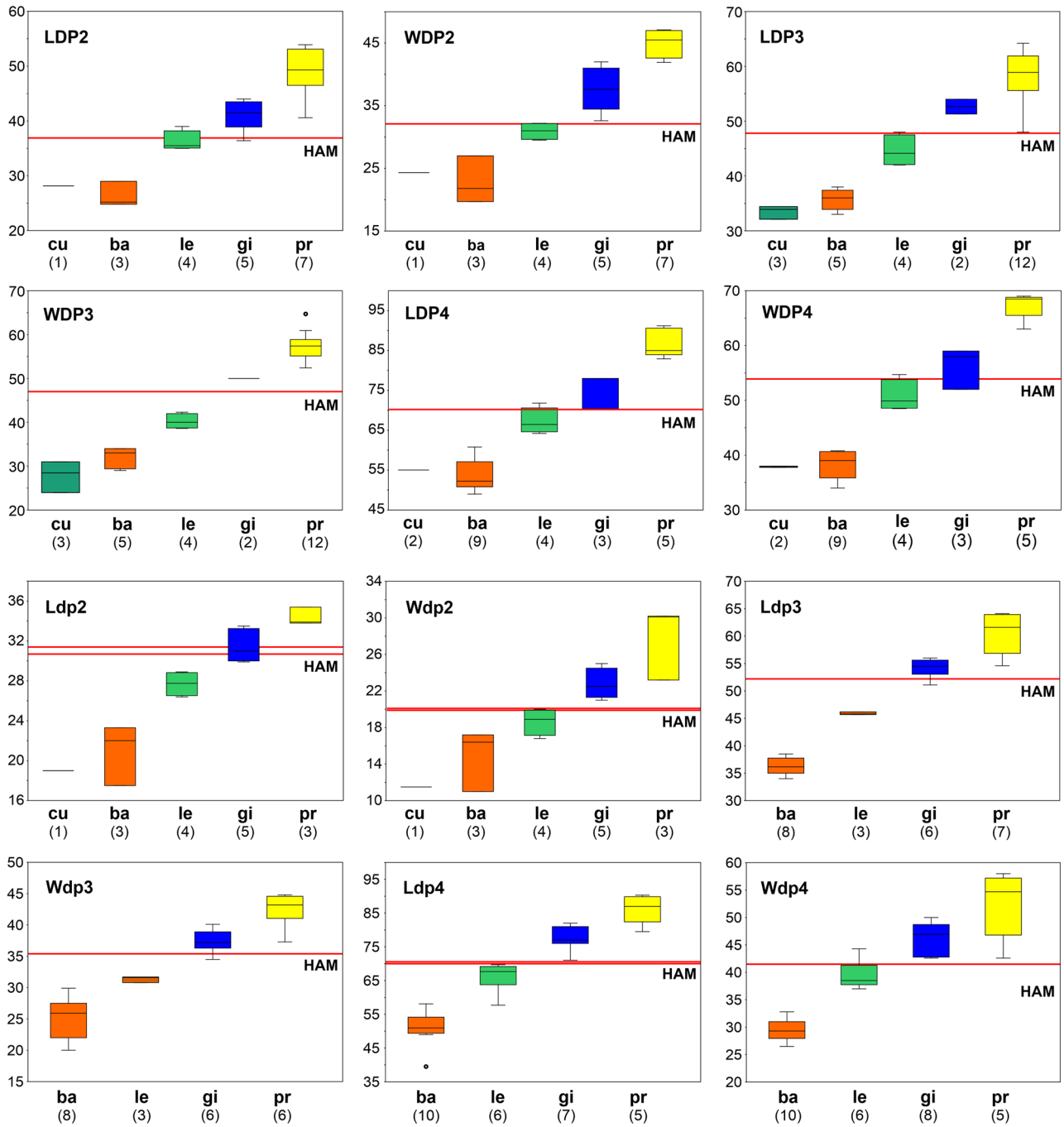

Fig. 8 Box-and-whisker plots of length (L) and width (W) (in mm) for the lower and upper deciduous premolars of European deinotheriid species compared to specimens from Hammerschmiede (red horizontal line). Black horizontal lines represent the median, boxes the 25 and 75 percentiles (interquartile range); whiskers the maximum-minimum values; circles the outliers; numbers in parentheses the number of specimens. Abbreviations: **cu,** *Prodeinotherium cuvieri*; **ba,** *Prodeinotherium bavaricum*; **le,** *Deinotherium levius*; **gi,** *Deinotherium giganteum*; **pr,** *Deinotherium proavum*. For the comparative sample see Table 3

specimens from Hollabrunn (Austria) and the similar-sized DP3 from Vetren (Bulgaria), both tentatively referred here to this species; see discussion below and Vergiev and Markov (2012)], while the WDP3 value stands between *D. levius* and *D. giganteum* (Figs. 7 and 8). The LDP4 value from HAM is plotted within the uppermost part of the intequartile range of *D. levius* and at the lower quartile of *D. giganteum*, while the WDP4 stands at the upper quartile of *D. levius* and the lower part of the intequartile range of *D. giganteum* (Fig. 8). The HAM DP4 plots together with the *D. levius* specimens

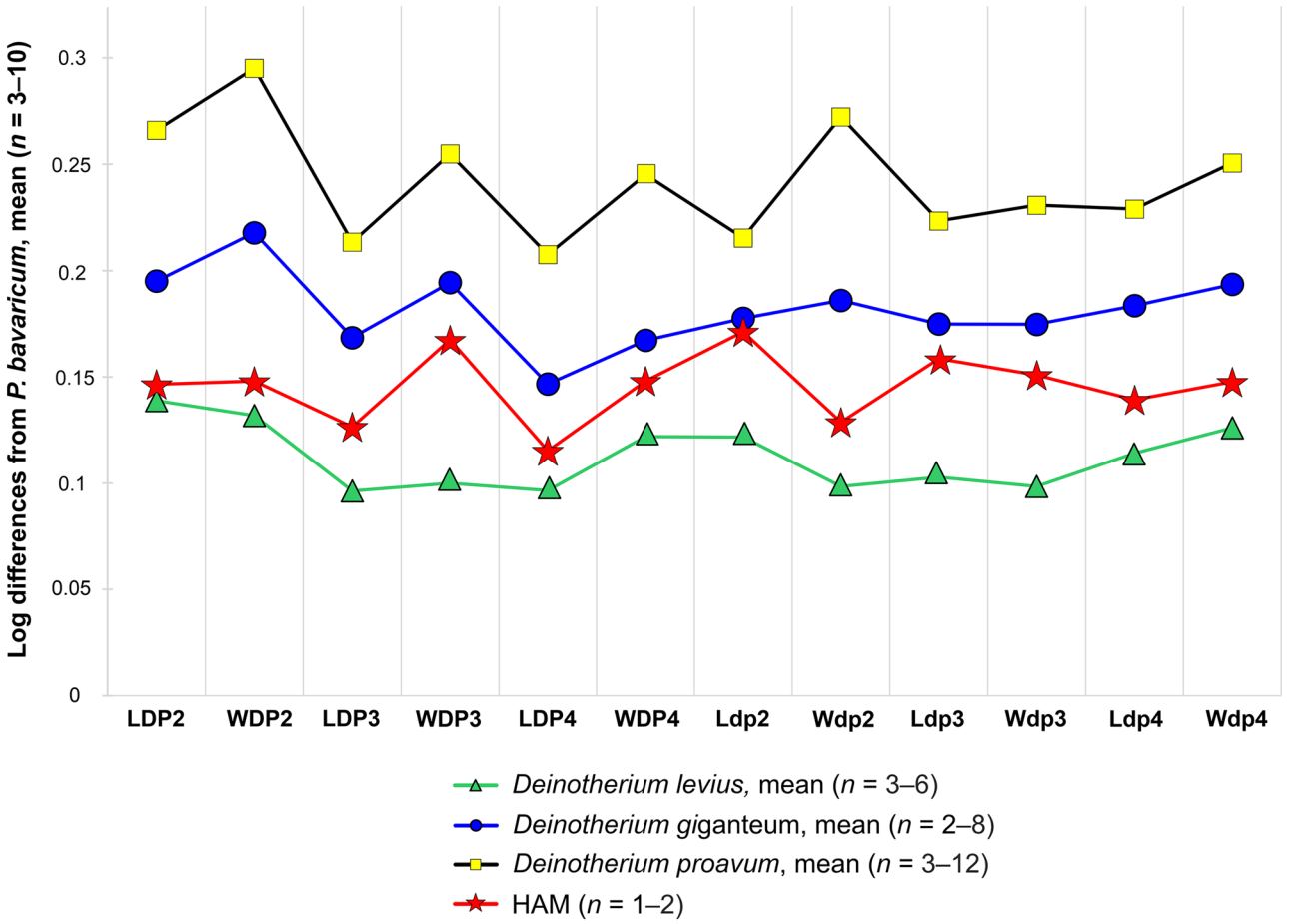

Fig. 9 Logarithmic ratio diagram comparing length (L) and width (W) of the lower and upper deciduous premolars from Hammerschmiede with *Deinotherium levius*, *Deinotherium giganteum* and *Deinotherium proavum* from various localities (see Table 3). Standard of comparison: mean values of *Prodeinotherium bavaricum*

from La Grive and Massenhausen, as well as with the single known DP4 from Montredon (France) (Figs. 7 and 8). The Ldp2 value from HAM is outside the range of *D. levius* and within *D. giganteum*, whereas the Wdp2 is outside the range of *D. giganteum* and at the upper quartile of *D. levius* (Fig. 8). The HAM dp2 is overall plotted close to the larger specimens from La Grive and the smaller ones from Montredon (Fig. 7). Both Ldp3 and Wdp3 values from HAM exceed the upper range of *D. levius* and are plotted at the lower range of *D. giganteum* (Fig. 8). The Ldp4 stands between *D. levius* and *D. giganteum*, while the Wdp4 values (CT-scan measurements) are at the upper quartile of *D. levius* (Fig. 8). The HAM dp4 is plotted close to the dp4 from Sopron [Hungary; the deinothere material from Sopron is attributed to *D. levius* by Aiglstorfer et al. (2014a)], the larger specimens from La Grive and Massenhausen, and the smaller one from Montredon (Fig. 7).

Similar results are obtained by the statistical comparison using z-scores of the HAM specimens with the *Prodeinotherium* and *Deinothereium* species from Europe. We must note, however, that the comparative sample for some species/tooth positions is insufficient, and therefore the results have to be considered indicative but treated with caution. The analysis detects significant differences of the HAM teeth for all tooth position and variables (except of Wdp2, and Wdp4 only for *D. proavum*) from *P. cuvieri*, *P. bavaricum* and *D. proavum* (Table 5). The HAM teeth are most similar with the Ldp4 and LDP3 (positive values) of *D. levius*, and the Ldp2, Ldp3 and Wdp3 (negative values) of *D. giganteum*, while they are within the variation of both these species for Wdp2, Wdp4, LDP2, WDP2, LDP4 and WDP4, for which variables however (except WDP4) the z-score is closer to zero for *D. levius*. Comparable results are acquired from the 95% confidence intervals for *D. levius* and *D. giganteum*, where the only differences compared to the z-scores is that in this case the HAM LDP2 is within *D. levius*, while the HAM LDP3 falls within both *D. levius* and *D. giganteum* (Table 5).

Morphological traits of the dp2 and DP2 provide further evidence for the taxonomic identification of the HAM specimens. Konidaris et al. (2017) and Konidaris and

Koufos (2019) noted that the morphology of the dp2, and in particular the position of the protoconid in regard to the metaconid, and the connection of the ectolophid with either of these cuspids, differs among the European deinotheriid species. In this aspect the HAM dp2 (Fig. 6n, q) is different from both *P. cuvieri* from Montréal-du-Gers (France; Ginsburg and Chevrier 2001: fig. 2l, m) where the proto- and metaconid are clearly separated, as well as from *D. proavum* from Pikermi (Greece; AMPG-PA3950/91) and Samos (Greece; SMF-M 3604), where the proto- and metaconid are fused, and the ectolophid is connected with the metaconid (Konidaris and Koufos 2019: fig. 4). HAM dp2 is also different from the dp2s of *D. giganteum* from Montredon (ML-MR- 52, FSL-210393), where the protoconid and the metaconid are almost or totally fused (Konidaris and Koufos 2019: fig. 4d, e). In *D. levius* from La Grive (ML-LGR 893, LGR 900, LGR 959; Ginsburg and Chevrier 2001: fig. 7) these cusps are either connected (but clearly distinct) or almost/totally fused and the ectolophid is connected with the protoconid. The best match of the HAM dp2s is with ML-LGR 893 of *D. levius*, where proto- and metaconid are located in a slightly more distant position (a primitive trait, not observed so far in *D. giganteum*).

The DP2 presents also some morphological differences among the European deinotheriid taxa (Konidaris et al. 2017; Konidaris and Koufos 2019). Based on these, the HAM DP2 (Fig. 6a) differs from that of *P. bavaricum* from Tavers, Pontlevoy (France, both MN 5) and Esselborn (Germany; HLMD-Din 237) in that the latter have a triangular shape due to the narrower protoloph in regard to the metaloph, resulting in the closer position of the proto- and paracone; a strongly curved crest that connects proto- and paracone (Stehlin 1925: fig. 21b; Ginsburg and Chevrier 2001: fig. 4b; Konidaris and Koufos 2019: fig. 4); and a relatively weak mesial projection of the mesial cingulum. On the other side, the DP2 of *D. giganteum* and *D. proavum* have a more rectangular shape, with an L-shaped connection of the proto- and ectoloph (Gaziry 1976; Sanders 2003; Garevski and Markov 2011; Konidaris and Koufos 2019; Fig. 4). The HAM DP2 matches with *D. levius* from La Grive ML-LGR 970, Massenhausen (SNSB-BSPG-1959 I 430) and Atzelsdorf (Göhlich and Huttenen 2009: pl. 1, fig. 1; Konidaris and Koufos 2019: fig. 4l, m), in which the crest connecting the protocone and paracone is curved (though less than *Prodeinotherium*), and these cusps stand in a more distant position to each other compared with *Prodeinotherium*, giving a trapezoid shape to the tooth due to the widening of the protoloph, while the mesial projection of the mesial cingulum is prominent.

Overall, the metric and morphological comparison reveals a clear distinction of the HAM deciduous teeth from *Prodeinotherium* spp. and *D. proavum*. Although the metric separation between *D. levius* and *D. giganteum* is not clear-cut for some deciduous teeth, the HAM specimens are for most tooth positions within the range of dimensions of *D. levius*, while additionally the morphology of the dp2 and DP2 matches best with *D. levius*. Therefore, we attribute the deinotheriid specimens from HAM to this species.

The shape and inclination of the mandibular symphysis (Fig. 4b, c) is also an important trait to be noted as it is shown that the symphysis of adult deinotheriid mandibles became evolutionary more ventrally inclined and contributes to the separation of species (see e.g., Gräf 1957: fig. 12). The mandibles SU-190 of *D. giganteum* from Nessebar (Bakalow 1914: pl. 1, 2; Bakalov and Nikolov 1962: pl. 42) and SMF-M 3604 of *D. proavum* from Samos (Konidaris and Koufos 2019) are ontogenetically comparable to the HAM mandible and their symphyses are stronger (note, however, that the Nessebar symphysis is partially reconstructed) and more ventrally inclined. Although the ontogenetic development (growth pattern) of the symphysis is unknown in deinotheres, due to the rarity of juvenile preserving this part, it seems that in addition to interspecific differentiation, the ontogenetic age is also of importance. For example, the mandible MGL-S 1048 of *D. proavum* from Samos (dp4 erupting), which is ontogenetically slightly younger than SMF-M 3604 (dp4 erupted), bears a less inclined symphysis than the latter specimen. Accordingly, the mandible from Isle-en-Dodon (MN 7, France; Lartet 1859: pl. 13, fig. 4; Duranthon et al. 2007) belonging to an older individual (m1 erupted) than HAM possesses a fairly deflected symphysis. Indeed, proboscidean mandibles are characterized by an evident intraspecific variability in morphology and dimensions affected mainly by the ontogenetic age, and these ontogenetic changes continue during the adult stages, when also sexual dimorphism influences the variation (e.g., Huttunen and Göhlich 2002; Tassy 2013; Álvarez-Lao and Méndez 2011). Therefore, for any taxonomic conclusion it is important to compare only mandibles of similar or at least approximate ontogenetic age.

Replacement of deciduous by permanent lower tusks in Deinotheriidae

Another important aspect of the deinotheriid partial juvenile skeleton from HAM 5 is the presence of juvenile lower tusks, both deciduous and permanent ones (Figs. 4d, f and 6j–m). The presence of deciduous lower tusks is well known in elephantimorphs (e.g., Tassy 1987; Göhlich 2010), but in more basal proboscideans, such as the deinotheriids, their presence is only scarcely documented. Following the criteria of distinguishing deciduous and juvenile permanent tusks (e.g., enamel cap with distinct cervix, closed pulp cavity; Tassy 1987) and the proposed tooth positions (Delmer 2009), we consider the lower tusk SNSB-BSPG-2020-XCV-0257

(Fig. 6j–m) to be deciduous (di1). This tusk was found in close spatial association (Fig. 2) with the juvenile mandible SNSB-BSPG-2020-XCV-0096 (the deciduous tusks may have become loose in the sockets and removed from the mandible soon after the death of the individual, like it may happen with elephants' upper tusks at the initial post-mortem stages during the decay of the carcass; Haynes 1988) whose symphysis preserves the emerging permanent lower tusks (Figs. 4 and 5), and therefore the isolated di1 and the mandible belong most possibly to the same juvenile individual (as also do the isolated right and left dp2s SNSB-BSPG-2020-XCV-0199 and 0092). Therefore, the HAM deinotheriid material not only provides another example of the possession of both deciduous and permanent tusks in deinotheres (Stehlin 1925: fig. 27; Harris 1976, 1983), but most importantly it captures the rare moment of transition between deciduous and permanent lower tusks in fossil proboscideans, a succession which corresponds to a short period of time during the early life of an individual, and to our knowledge it represents the first such well-documented example in deinotheriids.

Two juvenile mandibles (SU-190 and 191) of *D.* ?*ganteum* from Nessebar are important in this aspect for comparison. SU-190 (Bakalow 1914: pl. 1, 2; Bakalov and Nikolov 1962: pl. 42) lacks the dp2, but preserves the slightly worn dp3s, and the erupting, still inside their crypts, dp4s. Two laterally curved lower tusks are protruding from the ventrally deflected symphysis and are identified as the deciduous ones. Of approximate ontogenetic age is the juvenile mandible consisting of the specimens MGL-S 1048 and S 380 from "Adriano" of Samos Island (Greece; Konidaris and Koufos 2019: figs. 2g, h and 3c), which preserves the dp2 alveolus, the unworn dp3, the erupting dp4, and a partially broken lower tusk that most possibly corresponds to a deciduous one. The second and ontogenetically older mandible from Nessebar, SU-191 (Bakalow 1914: pl. 3, 4, 5, fig. 1; Bakalov and Nikolov 1962: pl. 43, fig. 1, a), bears the much-worn dp2s and dp3s, the slightly worn dp4s, and the erupting but still inside the alveolus, m1s. The two lower tusks that are preserved in the symphysis correspond in this case most possibly to permanent ones. Based on the tooth eruption and wear, the mandible of *Deinotherium bozasi* Arambourg, 1934 KNM-ER 354 from East Turkana (Kenya; Harris 1976: pl. 2b, 1983: pl. 2.3b, 2.4) belongs to an individual of comparable ontogenetic age and preserves the permanent lower tusks. The HAM mandible with the minimally worn dp2 (associated to the mandible) and dp3, the unworn dp4 that is not completely erupted, and with not preserved and most likely not formed m1, belongs to an individual of intermediate ontogenetic age between SU-190, and SU-191 and KNM-ER 354, and is perhaps close to KNM-ER 518 (Harris 1976: pl. 2c, 1983: pl. 2.3c). Therefore, the replacement of deciduous lower tusks by their permanent successors occurs around the time when the m1 is formed within the mandible, and the di1 is already shed when m1 is erupting.

Elephantimorpha Tassy and Shoshani in Shoshani et al., 1998
Elephantida Tassy and Shoshani in Shoshani et al., 1998
Gomphotheriidae Hay, 1922
Tetralophodontinae van der Maarel, 1932
Tetralophodon Falconer, 1857
Tetralophodon longirostris (Kaup, 1832a, b).

Type material: HLMD-Din 111 (holotype), left mandibular fragment with m2–m3; originally figured in Kaup (1835: pl. 19, figs. 1 and 2) and later in Tobien (1978: pl. 10, fig. 1).

Type locality: Eppelsheim, Germany, Miocene.

Material (HAM 5): left i2, GPIT/MA/13792; right dp4, GPIT/MA/12313; left DP3, GPIT/MA/12196; right P3, GPIT/MA/09554.

Material (HAM 6): right i2 (cast, original belongs to the private collection of M. Schmid, Marktoberdorf), GPIT/MA/19246; right m2, GPIT/MA/10800–03; right I2, GPIT/MA/10800–01; right M1?, GPIT/MA/10800–05; left M2, GPIT/MA/10800–04; right M3, GPIT/MA/10800–02; left m3 fragment (cast, original belongs to the private collection of M. Schmid, Marktoberdorf), GPIT/MA/19247; as well as numerous fragments of long bones and vertebrae (partial skeleton).

Description

Lower dentition The small-sized lower tusk GPIT/MA/13792 (total length: 54.8 mm) from HAM 5 has a rather oval cross-sectional shape (width: 10.9 mm; height: 15.0 mm), but with a longitudinal dorsal concavity (Fig. 10a, b). There is neither an enamel cap nor any other traces of enamel, but there is a small wear facet at the dorsomedial side of the tip.

The lower tusk (Fig. 10c–e) from HAM 6 is almost straight and its maximum preserved length is 440 mm; however, in its proximal part the tusk is roughly transversally broken, indicating that the original tusk was longer. The proximal cross-Sect. (64.1 × 50.8 mm; circumference: 180 mm) is subcircular and bears a shallow dorsal concavity, while ventrally it is convex. The Schreger lines that are visible in the cross-section form slightly acute angles of ~ 87–88° (Fig. 10c). The dorsal concavity runs longitudinally until the wear facet (ca. 110 mm in length and 41.8 mm in width), which is present at the dorsolateral side of the tip.

The dp4 GPIT/MA/12313 from HAM 5 exhibits four lophids (Fig. 11d–f). The mesial cingulum is damaged in its lingual part; in its labial part it is worn and connects with pretrite lophid 1. All lophids are worn, and the dentine is confluent on the pretrite and posttrite half-lophids. In lophid 1, the half-lophids are transeversely opposite to each other,

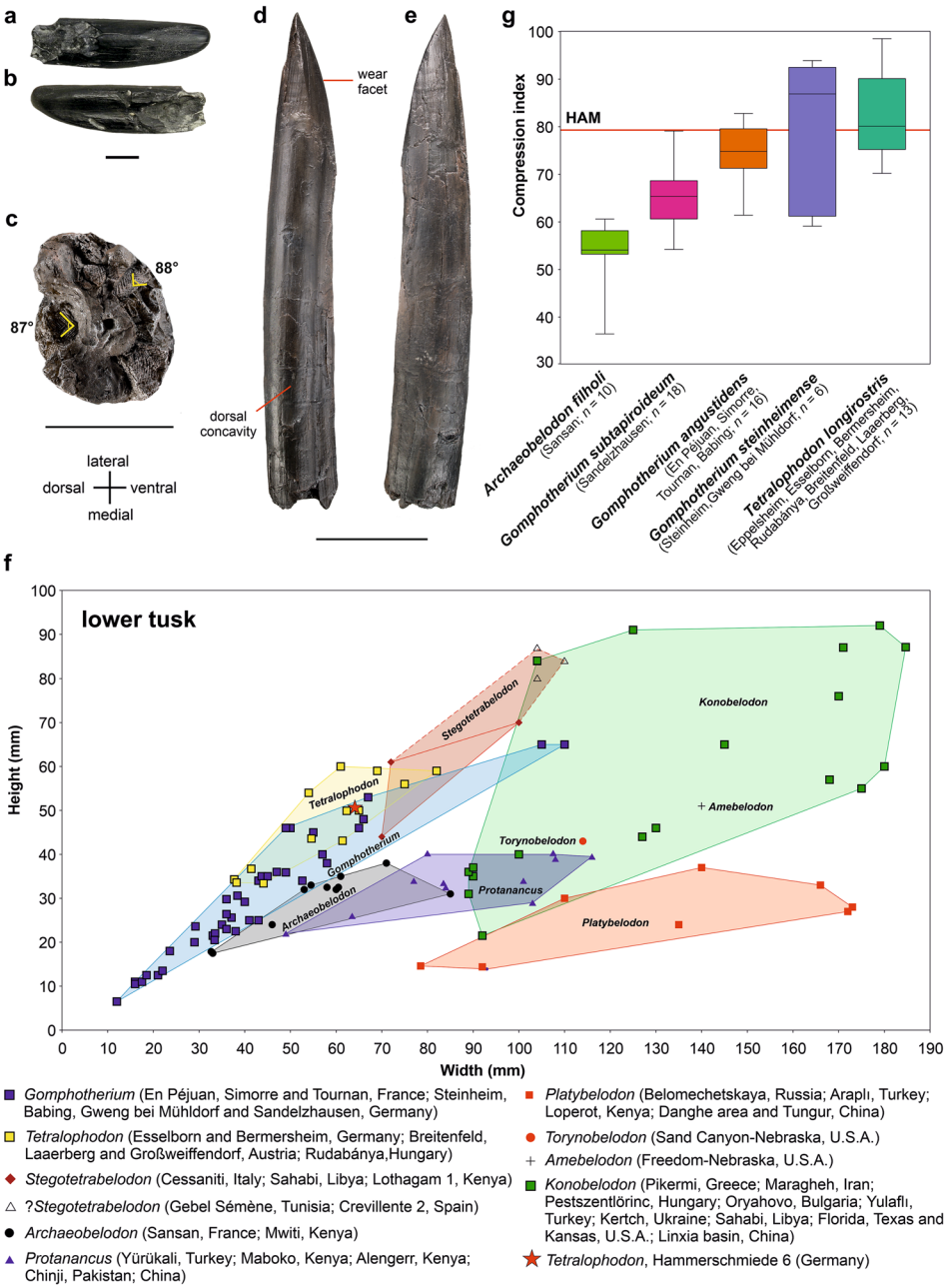

Fig. 10 Morphology and metric comparison of the lower tusks (i2) of *Tetralophodon longirostris* from Hammerschmiede. **a–b.** Left (juvenile permanent) i2, HAM 5, GPIT/MA/13792 in ventral (**a**) and dorsal (**b**) view. **c–e.** right (adult) i2 (cast), HAM 6, GPIT/MA/19246 in cross-sectional (**c**), dorsal (**d**) and ventral (**e**) view; in c the slightly acute Schreger lines are also shown. Scale bars equal 1 cm in a–b, 5 cm in c, and 10 cm in d–e. **f.** Bivariate plot (width vs. height) comparing the lower tusk of *T. longirostris* from Hammerschmiede 6 with lower tusks of various Miocene proboscideans. Note that the lower tusks belong to individuals of different ontogenetic ages and the location of the measurements differs among them (e.g., maximal preserved diameters if isolated or infront of the mandibular symphysis if embedded). The symbol '?' indicates incomplete or inadequately preserved specimens. Bivariate plot based on Konidaris and Tsoukala (2020: Fig. 5d, and references cited in the corresponding caption) plus Steininger (1965), Göhlich (1998, 2010) and Gasparik (2004); it is noted that the upper range for *Archaeobelodon* in the figure of Konidaris and Tsoukala (2020) was extended due to an oversight in the measurements. **g.** Box-and-whisker plot comparing the compression index of the lower tusks of *Archaeobelodon filholi*, *Gomphotherium* spp. and *Tetralophodon longirostris* from various localities with GPIT/MA/19246 from Hammerschmiede (red horizontal line); data from Klähn (1931), Steininger (1965), Mottl (1969), Tobien (1973), Göhlich (1998, 2010), Gasparik (2004), Tassy (2014), and own measurements at HLMD

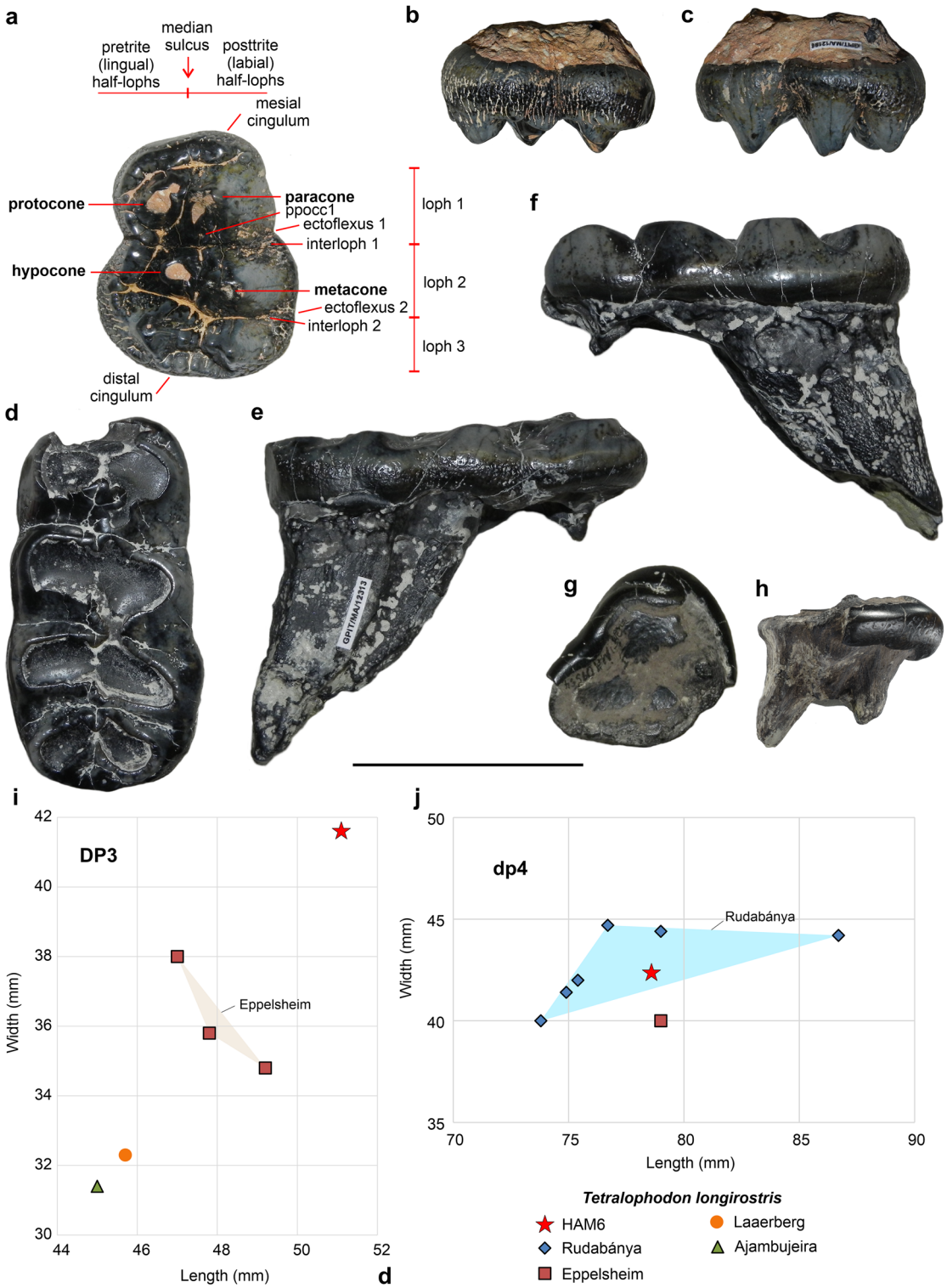

Fig. 11 Morphology and metric comparison of the third upper deciduous premolar (DP3), fourth lower deciduous premolar (dp4) and third upper premolar (P3) of *Tetralophodon longirostris* from Hammerschmiede. **a–c.** Left DP3, HAM 5, GPIT/MA/12196 in occlusal (**a**), (**b**) and (**c**) view. **d–f.** Right dp4, HAM 5, GPIT/MA/12313, in occlusal (**d**), labial (**e**) and lingual (**f**) view. **g–h.** right P3, HAM 5, GPIT/MA/09554 in occlusal (**g**) and labial (**h**) view. Scale bar equals 5 cm. **i.** Bivariate plot of length vs. maximum width (in mm) for DP3 of *T. longirostris* from various localities. **j.** Bivariate plot of length vs. maximum width (in mm) for dp4 of *T. longirostris* from various localities (see Table 4)

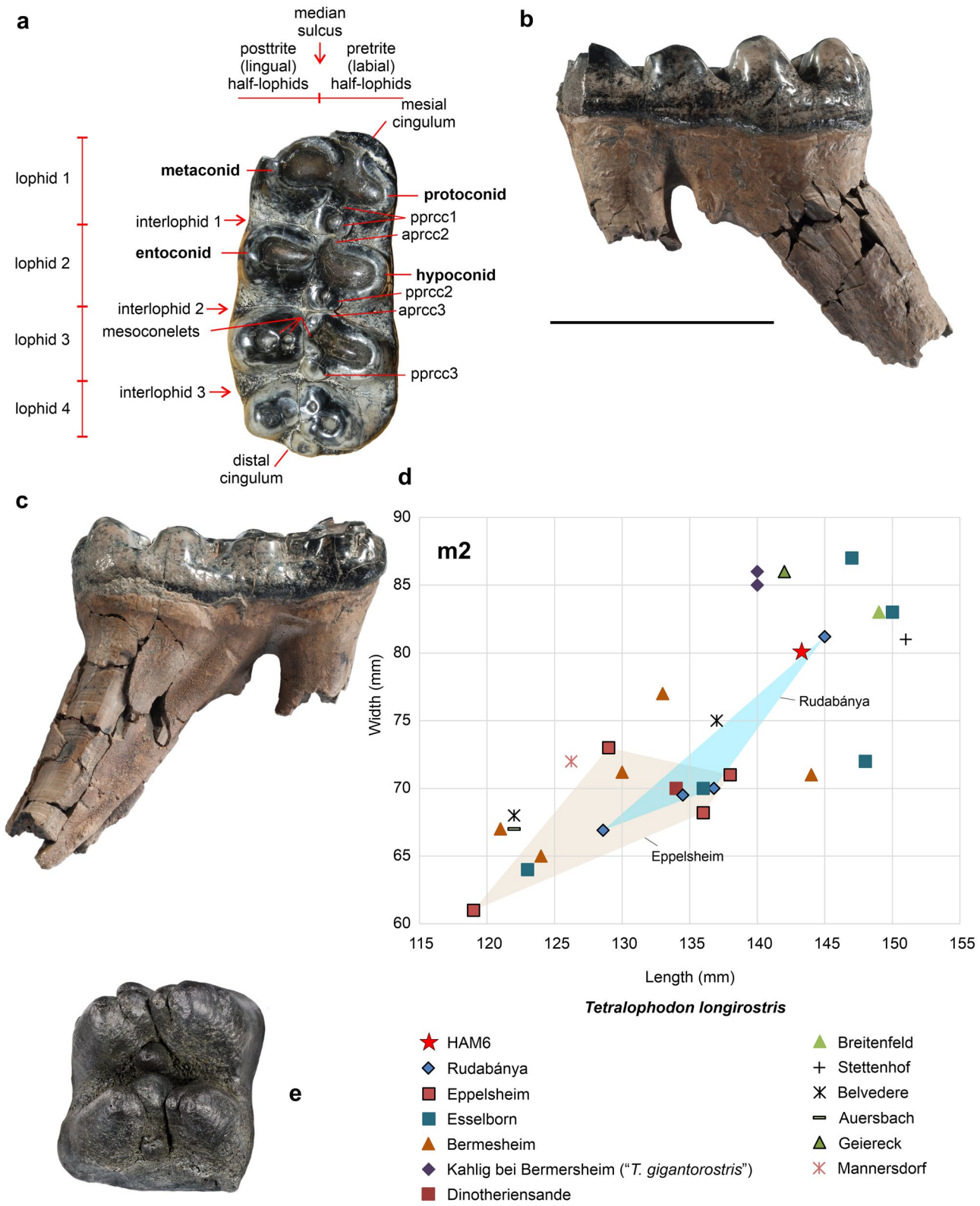

Fig. 12 Morphology and metric comparison of the lower molars of *Tetralophodon longirostris* from Hammerschmiede 6. **a–c.** Right m2, GPIT/MA/10800–03, in occlusal (**a**), lingual (**b**), and labial (**c**) view. **d.** Bivariate plot of length vs. maximum width (in mm) for m2 of *T. longirostris* from various localities (see Table 4). **e.** Left m3 fragment (cast; GPIT/MA/19247) of *Tetralophodon longirostris* from Hammerschmiede 6. Scale bar equals 10 cm

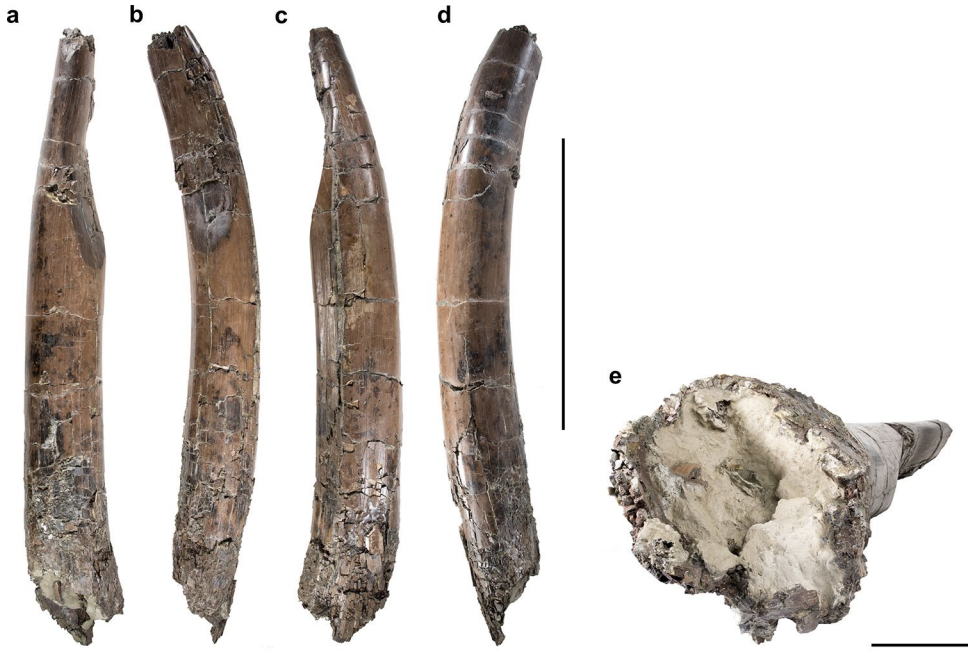

Fig. 13 Right upper tusk (GPIT/MA/10800–01) of *Tetralophodon longirostris* from Hammerschmiede 6 in ventral (**a**), medial (**b**) dorsal (**c**), lateral (**d**) and cross-sectional (**e**) view. Scale bars equal 50 cm in **a–d**, and 5 cm in **e**

whereas in lophid 2 and more pronounced in lophid 3 the pretrite half-lophids are set in a more diagonal position relative to the posttrite ones; in lophid 4, the half-lophids form a mesially pointed chevron structure. In interlophids 1 and 2, the larger pprcc1 and 2 abut the smaller aprcc2 and 3, respectively, blocking the labial sides of the interlophids; lingually the interlophids are open. A similar structure is visible in interlophid 3, but the pprcc3 is smaller than the corresponding ones of lophids 1 and 2. The distal cingulum is formed by three cuspules, of which the most pretrite one is the stronger and higher. The enamel is slightly corrugated towards the distal, and less worn, part of the tooth. The mesial root is damaged, while the two distal ones are fused.

The tetralophodont m2 from HAM 6 is very worn and dentine is exposed on all lophids (Fig. 12a–c). The mesial cingulum is damaged at its lingual part; at the labial part it is low but strong and is connected through the confluent due to wear dentine with pretrite half-lophid 1. Lophid 1 is very worn. There are two ppcc1, of which the more distal one is robust, labially blocking the interlophid 1and abutting the weak aprcc2. At the labial side of interlophid 1, there are remnants of cingulum. Lophid 2 is also very worn, but the two half-lophids are separated by the median sulcus. In interlophid 2, the strong (but slightly less than pprcc1) pprcc2 abuts the weaker aprecc3. In lophid 3, the pretrite half-lophid is set diagonal relative to the posttrite one. The latter bears two mesoconelets, of which the adaxial one is stronger. Interlophid 3 is blocked at its labial part by the pprcc3. In lophid 4, the two mesoconelets are set mesially relative to the main cusps. The distal cingulum consists of two cuspules, of which the labial one is higher and larger.

A middle fragment of a m3 (cast) from HAM 6 preserves two lophids (Fig. 12e). Each pretrite and posttrite half-lophid bears a mesoconelet, which on the pretrite side is in a slightly more mesial position in regard to the main cusp. This is more strongly expressed in the distal lophid. The preserved mesial lophid has one anterior and one posterior pretrite central conule, while the distal lophid only a weaker posterior one.

Upper dentition The upper tusk GPIT/MA/10800–01 (length arc: 1030; length chord: 920; circumference: 410; maximal diameters: 140 × 126 proximal; all in mm) from HAM 6 is ventrally curved, has an ovoid cross-section and lacks an enamel band (Fig. 13). In the proximal part, the pulp cavity is open (indicating that the tusk is almost completely preserved) and partially filled with sediment, while the distal part (tip) is missing. There is a long medial wear facet (maximal diameters wear facet: 370 × 104 mm).

The slightly worn DP3 GPIT/MA/12196 from HAM 5 is trilophodont with narrow loph 1, and wide lophs 2 and 3 (Fig. 11a–c). Mesially it shows a polished surface due to the contact with the DP2. The mesial cingulum is low, but strong, and consists of worn cusplets in a row. It continues and becomes high at the lingual side, and even stronger and higher at the level of loph 2. The cingulum ends at interloph 2. In loph 1, protocone and paracone are opposite to each other, but the latter is higher. The paracone bears a lower and worn mesoconelet set in a more distal position, as well as a low and worn posterior central conule. The protocone bears a similar in height mesoconelet, but it is directed mesially. Lophs 1 and 2 are separated by clearly marked ento- and ectoflexus. Interloph 1 is straight and open but closed

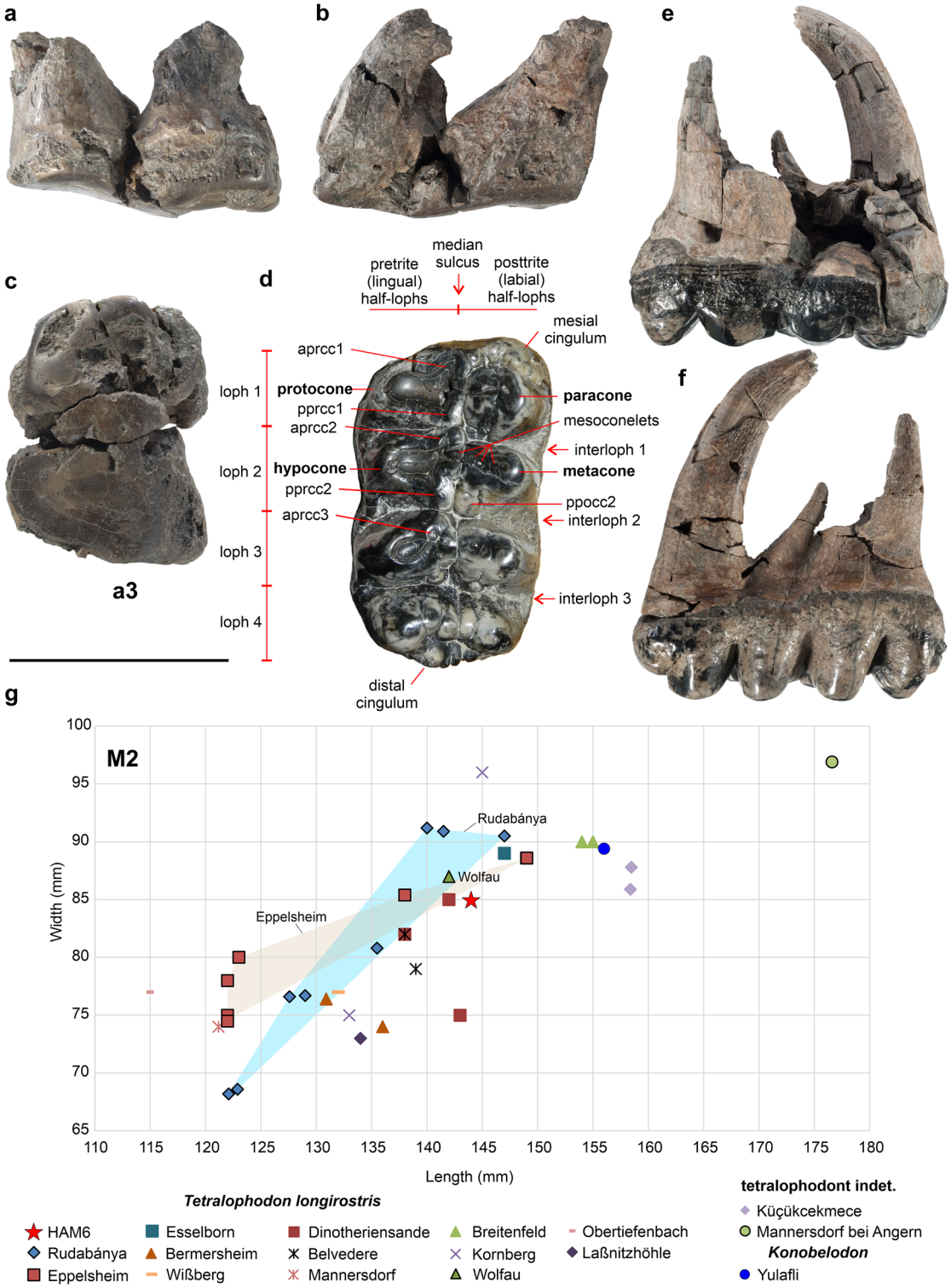

Fig. 14 Morphology and metric comparison of the first (M1) and second (M2) upper molars of *Tetralophodon longirostris* from Hammerschmiede 6. **a–c**. Right first upper molar? (M1?, GPIT/MA/10800–05) in lingual (**a**), labial (**b**) and occlusal (**c**) view. **d–f**. Left M2, GPIT/MA/10800–04, in occlusal (**d**), labial (**e**) and lingual (**f**) view. Scale bar equals 10 cm. **g**. Bivariate plot of length vs. maximum width (in mm) for M2 of *T. longirostris, Konobelodon* and tetralophodont indet. from various localities (see Table 4)

lingually by the strong cinglulum. Loph 2 is set diagonally. The metacone is higher than the hypocone and is fused with one mesoconelet; the hypocone and mesoconelet are worn and confluent. There is no second entoflexus and the second ectoflexus is very weak. The transverse valley is relatively sinuous and open, apart from the blocked by the cingulum lingual part. In loph 3, the posttrite main cusp is unworn and located in a more distal position relative to the slightly worn pretrite main cusp. The mesoconelets are lower than the main cusps. The distal cingulum is formed by four to five relatively low cusplets, which increase in height and strength towards the lingual side. The enamel is corrugated.

GPIT/MA/09554 from HAM 5 is a small-sized, deeply worn, tooth; it is of triangular shape with narrow mesial part and wider distal one (Fig. 11g, h). In its mesial part the enamel is thick, indicating that the specimen is not a deciduous premolar. The tooth is tentatively identified as a third upper premolar. There is a strong mesial cingulum which is connected to the pretrite side of the mesial loph. Enamel is missing from the distal side of the tooth.

GPIT/MA/10800–05 is a severely worn tooth (complete absence of enamel) from HAM 6, which is tentatively identified here as an upper M1 due to its length (116.2 mm), which is much smaller than the M2 GPIT/MA/10800–04 (144.0 mm) (Fig. 14a–c). The preservation of two single roots at the mesial part of the tooth indicate that no substantial loss of the original length could have happened although the advanced wear stage, excluding an identification as a M3. However, alternatively, it may be a smaller-sized M2.

The tetralophodont M2 from HAM 6 is relatively worn, and dentine is exposed in the first three lophs (Fig. 14d–f). There is a polished interproximal surface due to contact with the M1. The tooth is slightly damaged mesiolingually. On the mesiolabial side, the cingulum is low but strong. In loph 1, the paracone and one mesoconelet are fused. The pretrite half-loph is much worn and the dentine is confluent; however, the strong aprcc1 is connected to the mesial cingulum, while the pprcc1 and the aprcc2 are connected blocking interloph 1 lingually. On its lingual-most part there is a strong bulge, while on its labial side there is low and weak cingulum. In posttrite half-loph 2, there are three fused to each other mesoconelets in a slightly more mesial position than the metacone, and one ppocc2. Pretrite half-loph 2 is very worn, but at least one mesoconelet is visible. The pprcc2 abuts the aprcc3 in interloph 2; on its lingual-most part four rather strong cuspules are located. In loph 3, the mesoconelets are set mesially relative to the main cusps; there are three mesoconelets in the posttrite half-loph and at least one in the worn pretrite one. Interloph 3 is open, but there are two weak cuspules, one in the posttrite and one in the pretrite side. Loph 4 is almost straight; there are two pretrite mesoconelets and one posttrite. The distal cingulum consists of five cuspules, larger and higher towards the lingual side.

The two mesial lophs of the M3 from HAM 6 are completely worn and the dentine is confluent (Fig. 15a–c). However, the molar preserves the mesial roots indicating that there is no loss of additional mesial lophs, and therefore the M3 was comprised of five lophs. There are strong bulges in the labial side of interloph 1; weaker ones are located in interloph 2 and even weaker in interloph 3. In the lingual side, there are two low but strong cuspules in interloph 2, two very large ones in interloph 3, and one strong in interloph 4. In loph 3, the pretrite half-loph is set diagonal to the posttrite one; it bears one strong aprcc3. In lophs 4 and 5, the mesoconelets (one for each half-loph) are positioned more mesially than the main cusps. Besides these mesoconelets, there is one very strong additional one located at the middle of the lophs, which is larger than the main cusps. The distal cingulum consists of three cuspules, of which the most lingual one is the strongest, while at the distal-most part of the tooth there are three additional weak cuspules.

Remarks

Tetralophodon encompasses tetralophodont gomphotheres with a long mandibular symphysis, pyriform to oval in cross-section lower tusks (in contrast to the brevirostrine and tuskless *Anancus*) that consist of concentric lamellar dentine (no dentinal rods like the amebelodontid *Konobelodon*), intermediate and third molars that show trefoil wear patterns (not plate like pattern such as the elephantid *Stegotetrabelodon*) and rounded upper tusks that lack enamel bands (Konidaris and Tsoukala 2022). In Europe, *Tetralophodon* is represented by its type species *T. longirostris*, the known biostratigraphic distribution of which ranges from the late Astaracian (MN 7/8; Middle Miocene) to the late Vallesian (MN 10; Late Miocene) (Tassy 1985). The type locality of *T. longirostris*, Eppelsheim, belongs to the Eppelsheim Formation ("Dinotheriensande") of the Mainz Basin in Germany, from where most of the known specimens originate. Originally, the tetralophodont proboscidean remains from "Dinotheriensande" were allocated by Kaup (1832b) to the species *Tetracaulodon longirostre* (*Tetracaulodon* is now regarded as a junior synonym of *Mammut*); slightly later (Kaup 1835) they were assigned to *Mastodon longirostris*, a species that was subsequently included within the subgenus *Mastodon* (*Tetralophodon*) by Falconer (1857). Besides *T. longirostris*, several other taxa have been proposed in the past based on material from "Dinotheriensande", e.g., *Mastodon grandis* Kaup and Scholl, 1864, *Mastodon wahlheimensis* Klähn, 1922, *Mastodon esselbornensis* Klähn, 1922, *Mastodon gigantorostris* Klähn, 1922, *Tetralophodon curvirostris* Bergounioux and Crouzel, 1960, mainly

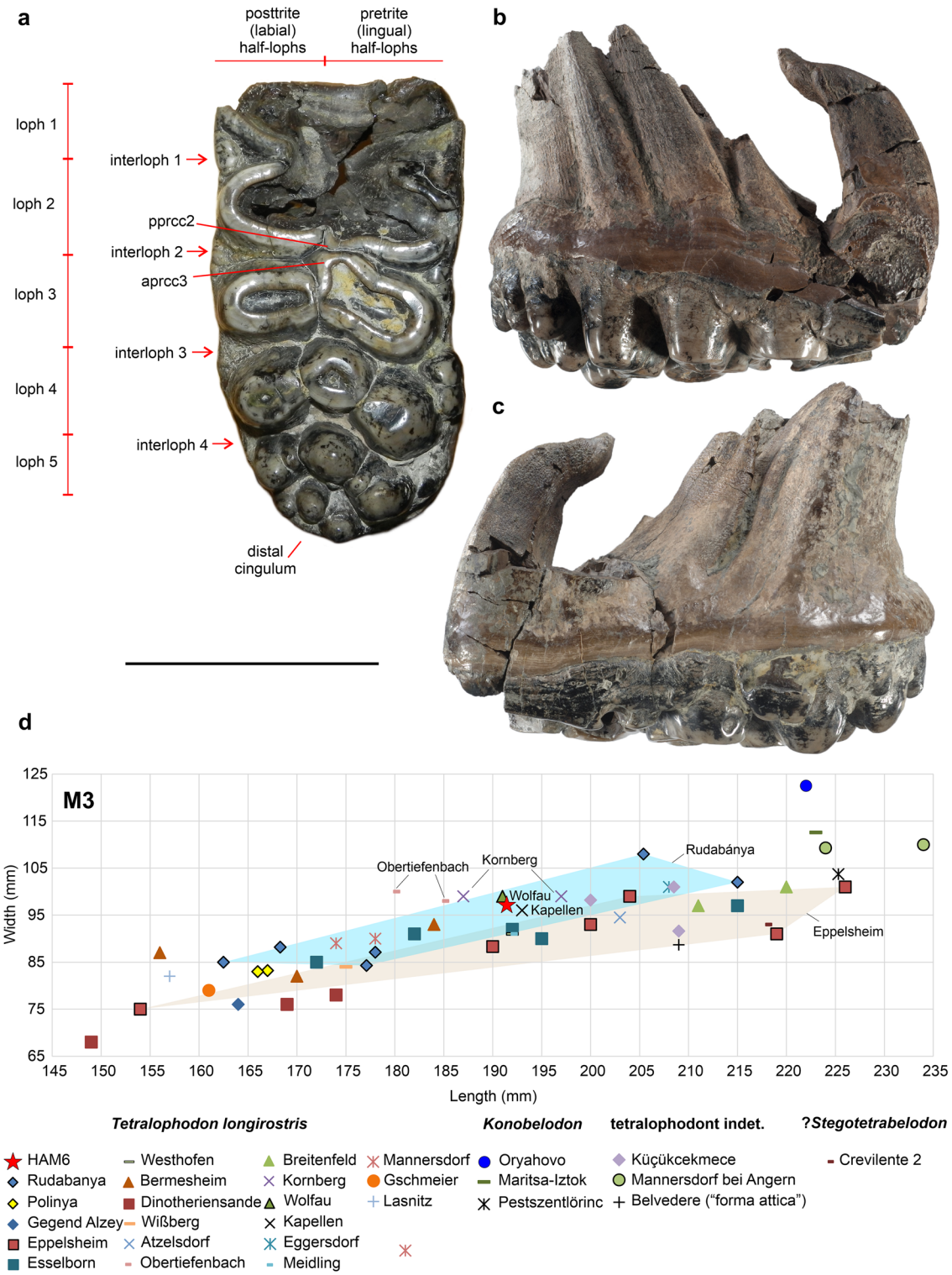

Fig. 15 Morphology and metric comparison of the third upper molar of *Tetralophodon longirostris* from Hammerschmiede 6. **a–c.** Right M3, GPIT/MA/10800–02, in occlusal (**a**), lingual (**b**) and labial (**c**) view. Scale bar equals 10 cm. **d.** Bivariate plot of length vs. maximum width (in mm) for M3 of *T. longirostris*, *Konobelodon*, tetralophodont indet. and ?*Stegotetrabelodon* from various localities (see Table 4)

on the grounds of dental size, and mandibular and dental and morphology. However, these species are considered junior synonyms and within the intraspecific variation (polymorphism) of *T. longirostris* (Tobien 1980; Tassy 1985, 1999). "Dinotheriensande" were generally considered to be of Vallesian age; however, recent studies indicate the stratigraphic inhomogeneity due to reworking of the sediments and a chronological range of the fauna from the Middle to the Late Miocene (Böhme et al. 2012; Pickford and Pourabrishami 2013). Taking also into account that, as in several historical collections, the fossils lack precise stratigraphic information, the revision of all known material from Europe and the discovery of new specimens with certain stratigraphic context are necessary to clarify the taxonomy and evolution of *Tetralophodon* from Europe.

Comparison

The combination of several morphological and metric traits, exclude the allocation of all HAM specimens to the trilophodont elephantimorphs *Archaeobelodon*, *Protanancus*, *Platybelodon*, *Choerolophodon* and *Gomphotherium*, as well as to the mammutids *Zygolophodon* and *Mammut*. In particular:

- Trilophodont DP3, tetralophodont dp4, m2 and M2, and five lophs with a distal cingulum in the M3, indicate that all HAM cheek teeth belong to a tetralophodont elephantimorph. Even the later and larger *Gomphotherium* (cf.) *steinheimense* (Klähn, 1922) (e.g., Steinheim, Massenhausen, Gweng bei Mühldorf; Germany) possesses M3 with four lophs that may bear a developed cingulum or 4 ½ lophs (Göhlich 1998; Göhlich and Huttunen 2009), but not five lophs.
- The absence of an enamel band (a derived trait) in the upper tusk from HAM further corroborates the exclusion of a more basal bunodont elephantimorph (see e.g., Tassy 2014), while an attribution to *Choerolophodon*, which also lacks an enamel band is ruled out, because this genus is characterized by strongly curved and double-twisted upper tusks (e.g., Konidaris and Koufos 2016).
- The subcircular cross-section of the lower tusk from HAM 6 combined with the presence of only concentric lamellar dentine in the inner part clearly precludes an attribution to the amebelodontid *Platybelodon*, whose lower tusks bear tubular dentine and are dorsoventrally strongly compressed (Fig. 10f). The lower tusks of the other amebelodontids *Protanancus* and *Archaeobelodon* are also more dorsoventrally compressed than the HAM specimen (Fig. 10f, g). On the other hand, the morphological and metric distinction with *Gomphotherium* is more difficult as the lower tusks of *Gomphotherium* and *Tetralophodon* are morphologically close and partially overlap metrically (Fig. 10f, g). The HAM lower tusk is distinct from *Gomphotherium suptapiroideum* (Schlesinger, 1917). In terms of the Ci, it stands at the upper quartile of *Gomphotherium angustidens* (Cuvier, 1817), and within the interquartile range of *Gomphotherium steinheimense* (Fig. 10g). However, the lower tusks of *G. angustidens* are mostly pyriform in cross-section (Tassy 2014: fig. 24), while those of *G. steinheimense* are circular in cross-section (Steinheim; Klähn 1931: pl. 2, fig. 1) or much larger (*G.* cf. *steinheimense*; Gweng bei Mühldorf; Göhlich 1998). The lower tusks of the zygolophodonts *Zygolophodon* and *Mammut* differ also from the HAM specimen by their oval cross-section (Tobien 1996).

On the other hand, tetralophodont elephantimorphs of Europe include *Tetralophodon*, *Anancus*, *Konobelodon*, *Stegotetrabelodon* and the "Crevilente 2 taxon" from Spain. Although the elephantid *Stegotetrabelodon* (present in Europe so far only in the region of Calabria in Southern Italy, which at that time was a northern extension of the African continent; Ferretti et al. 2003) retains some gomphothere traits, it differs from the HAM specimens in the straight and not ventrally curved upper tusks, the pentalophodont (or almost) m2/M2, and the equal development of the cusps which are aligned forming a plate-like pattern (Tassy 1999). These elephantid traits are also present in the molars of the derived tetralophodont taxon from the Turolian of Crevillente 2 (Spain), originally attributed to *Tetralophodon* cf. *longirostris* 'grandincisivoid form', but with possible *Stegotetrabelodon* affinities (Mazo and Montoya 2003; Mazo and Made 2012; Tassy 2016). Additionally, the not completely preserved M3 of this taxon (Mazo and Montoya 2003: pl. 7, figs. 1 and 2) shows six lophs and is characterized by a multiplication of cusps, while its dimensions are larger than the HAM M3 (Fig. 15d). An attribution of the HAM cheek teeth to *Anancus* can also be excluded because this genus [including the earliest representative from the Late Miocene of Europe *Anancus lehmanni* (Gaziry, 1997)] is characterized by the dislocation of the pretrite and posttrite half-loph(id)s, which results in the alternate arrangement of the successive loph(id)s (anancoidy), a feature not present on the studied specimens, while this genus is equipped with almost straight upper tusks and does not bear lower tusks (Tassy 1986; Hautier et al. 2009; Konidaris and Roussiakis 2019). The other tetralophodont candidate is the tetralophodont amebelodontid *Konobelodon*, represented in Europe by *Konobelodon atticus* (Wagner, 1857). The latter is diagnosed among others by its enlarged loph 3 in the DP3 with well-marked second ento- and ectoflexus, and by large-sized, dorsoventrally flattened lower tusks bearing internally tubular dentine (Fig. 10f; Konidaris et al. 2014; Konidaris and Tsoukala 2020, 2022); on the contrary, in the HAM DP3 loph 3 is short, there is no entoflexus 2, the ectoflexus 2 is weak, while the lower tusk is subcircular, is formed only by

concentric dentine and is of smaller size (Figs. 10c, f and 11a). Additionally, the dimensions of the known M2, M3 of European *Konobelodon* (e.g., Pestszentlörinc, Hungary; Oryahovo, Maritsa Iztok, Bulgaria; Yulafli Turkey; and perhaps Mannersdorf bei Angern, Austria), and the M2 and M3 from Küçükcekmece (Turkey), attributed to "tetralophodont form, gen. and sp. indet." (Tassy 2016) are larger than the HAM specimen (Figs. 14g and 15d).

On the other hand, the HAM specimens match well with *Tetralophodon longirostris*. In particular (based on Tassy 1985: p. 723–724):

- Trilophodont DP3, tetralophodont intermediate molars, and M3 with five lophs (Figs. 11, 12, 14, 15).
- Tetrabelodont with rounded upper tusk lacking an enamel band, and subcircular/pyriform lower tusk with a dorsal concavity and without a ventral one (Figs. 10a–e, 13).
- Alternate contact (posttrite-pretrite) between the two mesial lophs (a derived trait) in the DP3 (Fig. 11a). The HAM specimen is morphologically similar to corresponding specimens of *T. longirostris* from Eppelsheim (HLMD-Din 1062 and casts MNHN-268, A.C. 1987; Kaup 1835: pl. 16, fig. 1a, pl. 17, fig. 12, pl. 20, fig. 2), Stierlingsandgrube am Geiereck (Laaerberg, Austria; Schlesinger 1917: pl. 12, fig. 1) and Azambujeira (Portugal; Antunes and Mazo 1983: pl. 1 fig. 6), in which loph 3 is not enlarged, ectoflexus 2 is weak (more marked in HLMD-Din 1062), and entoflexus 2 is absent or not very marked. Nonetheless, the HAM DP3 is larger than all other known *T. longirostris* specimens (Fig. 11i).
- Asymmetry in the pretrite trefoils with smaller posterior central conules compared to the anterior ones in the M3 (Fig. 15a).
- In the lophs distally of loph 3 in the M3, the mesoconelets are shifted mesially, and are as high as the main cusps of the loph (Fig. 15a).

However, within *T. longirostris* there are certain variable features in the last molars, the main of which relate to the complexity of the occlusal morphology, the crown dimensions, and the number of loph(id)s, as well as differences in the size, shape and Ci of upper/lower tusks.

Size, cross-sectional shape and compression index of upper/lower tusks The size, cross-sectional shape and Ci of the adult HAM 6 lower tusk match well with *T. longirostris* (Fig. 10c–g). However, the known *T. longirostris* lower tusks vary in size, cross-sectional shape and CI. The cross-section is roughly rounded (and accordingly the Ci is close to 100) in the Esselborn (HLMD-Din 1087; L tusk protruding from the symphysis = 320 mm) and Bermersheim (L tusk protruding from the symphysis = 700 mm; Klähn 1931) lower tusks, whereas it is reported as pyriform in the Breitenfeld specimen (Mottl 1969). The Ci of the tusks from Rudabánya ranges from 70.2 (the lowest value for the species *T. longirostris* in general) to 91.0 highlighting the great variability within a sample. In terms of size and Ci, the HAM tusk fits best with Laaerberg and HGI-V.11953 from Rudabánya, while in terms of cross-sectional shape is close to the Grossweissendorf specimen (Austria; Steininger 1965) and HLMD-Din 999 from Eppelsheim. The general morphology is also similar with the specimen from Breitenfeld (Mottl 1969: pl. 1, fig. 2).

Only few upper tusks of *T. longirostris* are known. The upper tusk from HAM has a similar morphology but is larger than one from Rudabánya [Hungary; maximal diameters cross-section: 123 × 114 mm; Gasparik, 2004, 2005; originally attributed to "*Tetralophodon*" *gigantorostris* (Klähn, 1922), see below), as well as from one from Belvedere (Austria; maximal diameters cross-section: 122 × 100, circumference: 352 mm; Schlesinger, 1917: pl. 19, fig. 2; Göhlich, 1998). On the other side, the length and cross-sectional dimensions are very close to the specimen from Villavieja del Cerro (Spain; 920 mm and 142 × 127 mm, respectively; Mazo and Jordá Pardo 1997). In terms of length, the HAM tusk is similar to the Polinya (Spain; 950 mm) one, with which it shares a similar general morphology (Alberdi 1971: pl. 2, figs. 3 and 4). Two more upper tusks are known preserving the distal part, one comes from Eppelsheim (HLMD-Din 998) and is figured in Kaup (1835: pl. 3, fig. 2) and the other from Altmannsdorf (Austria) described in Schlesinger (1917: pl. 12, fig. 4).

Complexity of the occlusal morphology Tetralophodont molars vary greatly in the complexity of their occlusal morphology, e.g., pretrite central conules may be weak or strong, posttrite central conules may be present or not, alternating contacts may be present or absent, while in addition the degree of complexity may vary among the upper and lower molars of the same individual, within the toothrow (e.g., M2–M3) or even between the mesial and distal part of a single tooth (Tassy 1985: p. 735; Metz-Muller 1995; Göhlich 1998: p. 88; Hautier et al. 2009). This is also the case for *Tetralophodon longirostris*, e.g., within the samples from Rudabánya and Eppelsheim. Therefore, the complexity of the molars, at least in small samples where the degree cannot be statistically evaluated, cannot be of taxonomic significance and provide evolutionary conclusions.

The HAM 6 m2 is much worn but shows a relatively simple structure, with the complex traits pertaining to the presence of a ppocc1 and pprcc3. The M2 shows a slightly more complex pattern, showing compressed posttrite

mesoconelets in lophs 2 and 3, as well as two ppocc2 and two cuspules (posttrite and pretrite) in interloph 3. The mesial lophs in the HAM M3 are worn and thus the degree of complexity cannot be observed; in the rest of the tooth the complexity of the occlusal morphology can be regarded as relatively simple (e.g., absence of posttrite central conules), but with additional weak to strong cusplets present in the lingual and labial sides of the interlophs. The HAM molars differ from the complex ones such as the M2 from Gars (SNSB-BSPG-1974 I 342) and the M3 from Atzelsdorf that show heavy ornamentation with multiplication of the conelets and the central conules (however, particularly in the mesial lophs that are not observable in the HAM molar). Another difference with the Atzelsdorf molar is that the latter bears in its distal half equal size main cusps and mesoconelets, whereas on lophs 4 and 5 of the HAM M3 there are particularly strong conelets in the central parts of the lophs.

Size variation Proboscideans are characterized by variation in the size of their molars, especially of the m3/M3, evident when large samples from a single site are available. Particularly informative is the sample of *G. angustidens* from the Middle Miocene (Astaracian) of En Péjuan (France). The studies of Tassy (1996b, 2014) proved that the size variation in the m3/M3 from a single site should be attributed primarily to sexual dimorphism and not to the presence of two species, concluding that in most cases small-sized gomphotheriid molars from the Miocene correspond to female individuals and not to small-sized species. On the other hand, size variation between distant population of the same species might be a response to local environmental factors reflecting thus differences at population level (Tassy 1996b).

Another example might be *Mastodon gigantorostris* of Klähn (1922) [or *Mastodon longirostris* forma *gigantorostris* in Klähn (1931)] from Kahlig bei Bermersheim (Dinotheriensande, Germany), a taxon which was later included in *Tetralophodon* by Osborn (1936) and in *Stegotetrabelodon* by Tobien (1978, 1980), followed also by Gaziry (1994). Besides some differences in the morphology of the holotypic mandible (mandibular angle, symphysis, and position of condyle in respect to the coronoid process), the main differences from *T. longirostris* are the more complicated structure, the presence of cement and the larger size of the molars (Klähn 1922, 1931; Tobien 1978, 1980; Gaziry 1994). According to Tassy (1985, 1999), however, this taxon is part of the polymorphism observed in European *T. longirostris*, while Göhlich (1999) notes that it is similar, if not identical, to *T. longirostris*. In this aspect, the rich tetralophodont material from Rudabánya plays an important role. The material consists primarily of isolated teeth, while unfortunately the preserved mandibles are fragmentary (and thus no comparison with the mandible of *Mastodon gigantorostris* is possible). The tetralophodont assemblage was separated into two species based mainly on size, *T. longirostris* and "*T.*" *gigantorostris* (Gasparik 2005). Indeed, the size range of the six preserved M3 is wide, which in Fig. 15d results into two clusters (see also Fig. 16). Such size variation is observed also in the m3 (Konidaris et al. 2014: fig. 7). However, this might be part of the intraspecific size variation of *T. longirostris* reflecting sexual dimorphism. The material from Dinotheriensande localities (e.g., Eppelsheim, Esselborn), part of historical collections, lacks precise stratigraphic information and cannot be regarded as homogenous, however, it also shows evident size variability (Figs. 15d and 16).

The m2 from the HAM 6 individual is plotted at the upper range of *T. longirostris* (Fig. 12d) close to the m2s from Kahlig bei Bremersheim (Germany; holotype of *Mastodon gigantorostris*), HGI-M.93.7 from Rudabánya ("*T.*" *gigantorostris* in Gasparik 2005), Stierlingsandgrube am Geiereck (Laaerberg; *Stegotetrabelodon grandicisivus* in Tobien 1978), Breitenfeld, Stettenhof (Austria), and to the larger specimens from Esselborn (HLMD-Din 856 and 1067) and Bremersheim (HLMD-Din 1072). For both Lm2 and Wm2 the HAM 6 m2 is plotted above the upper quartile of Rudabánya and Dinotheriensande (Fig. 16). Likewise, the M2 from HAM 6 is also plotted at the upper range of *T. longirostris* (Fig. 14g) close to the M2 from Wolfau (Austria), and to the larger specimens from Rudabánya ("*T.*" *gigantorostris* in Gasparik 2005), Eppelsheim (HLMD-Din 770), Esselborn (HLMD-Din 755), "Dinotheriensande", and Kornberg (Austria; LMJ 60.114; in terms of length). The HAM 6 LM2 stands above the upper quartile of Rudabánya and Dinotheriensande, while the WM2 at the upper part of the interquartile range of the former locality and at the upper quartile of the latter (Fig. 16). The M3 from the same HAM 6 individual is plotted roughly at the middle of the size variation of *T. longirostris* (note that the maximum length is likely affected by the advanced wear at the mesial part and thus it may be slightly an underestimate of the original, unworn, one), close to the M3s from Kornberg, Wolfau, Meidling (Austria), Kapellen (Slovenia; Bach 1910), Westhofen (Germany), and to HLMD-Din 751 from Esselborn (Fig. 15d). For both LM3 and WM3 the HAM 6 M3 is plotted at the upper part of the interquartile range of Rudabánya (separation into male and female individuals is possible) and Dinotheriensande, (Fig. 16). Overall, the HAM 6 T. *longirostris* belongs to a large-sized individual (probably male; see remarks below).

Number of loph(id)s The HAM 6 M3 is formed of five lophs, of which the last one is short and is accompanied by a rather reduced distal cingulum (Fig. 15a). This occlusal pattern differs from M3s of *T. longirostris* that consist of 4–4 ½ lophs, such as Obertiefenbach bei Fehring (Austria; Bach 1910: p. 66, pl. 7, fig. 14), Bermersheim (HLMD-Din 600) and Atzelsdorf (Göhlich and Huttunen 2009; *T.* cf. *longirostris*). It also differs from specimens having a wide loph

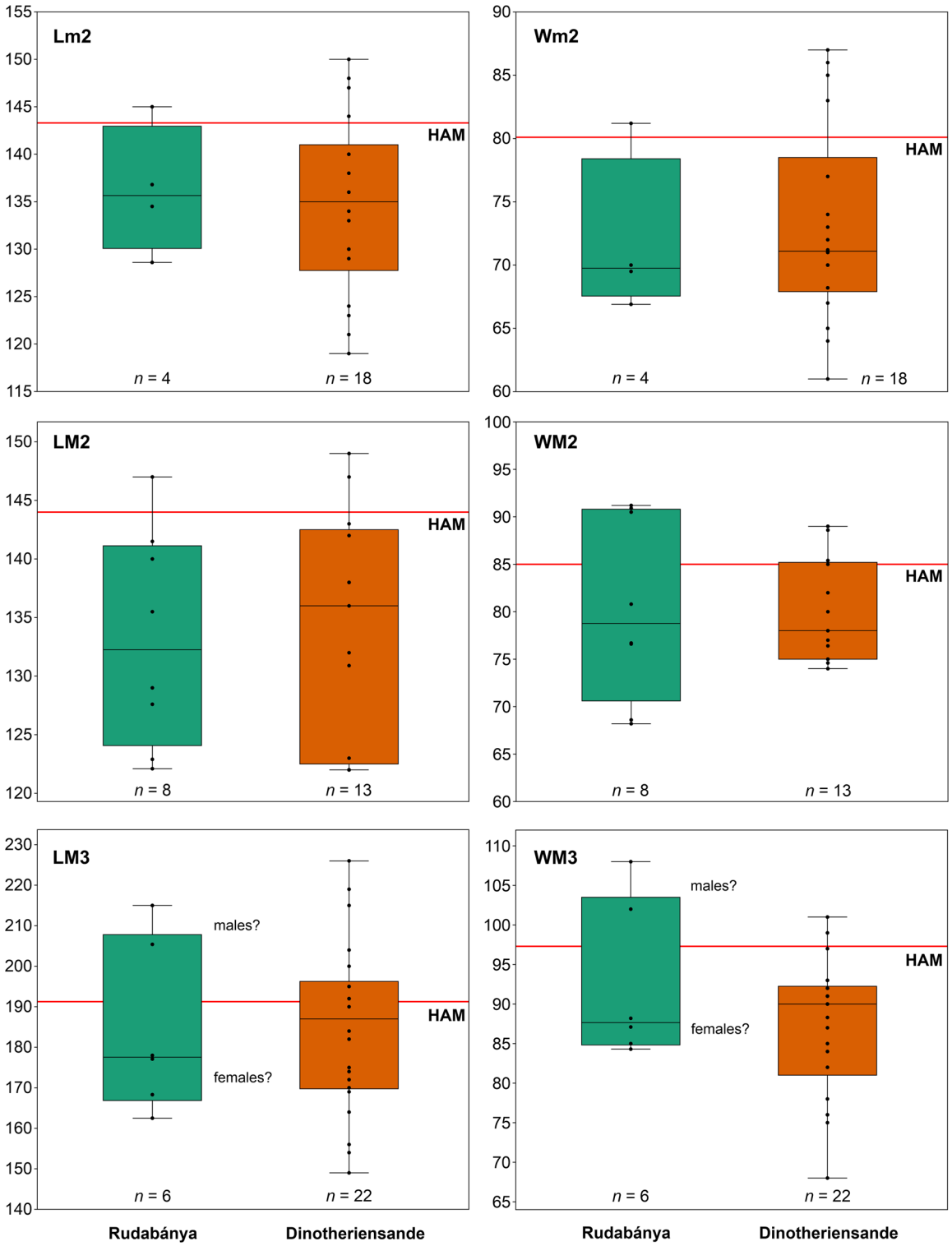

Fig. 16 Box-and-whisker plots of length (L) and width (W) (in mm) for the m2, M2 and M3 (specimens appear with black dots) of *Tetralophodon longirostris* from Rudabánya (Hungary) and from Dinotheriensande (Germany) sites compared to the specimens from Hammerschmiede (red horizontal line). For explanation see Fig. 8 and for the comparative sample Table 4

5, e.g., HLMD-Din 751 from Esselborn (Gaziry 1994: pl. 2, fig. 5) or even a sixth loph, e.g., HLMD-Din 651 from Eppelsheim (Gaziry 1994: pl. 3, fig. 3). The HAM M3 is comparable with HLMD-Din 757 from Wißberg (Germany; Gaziry 1994: pl. 2, fig. 6), HLMD-Din 759 from Westhofen (Gaziry 1994: pl. 2, fig. 4), and the molars from Kapellen (Bach 1910: pl. 10, fig. 2) and Eggersdorf (Austria; Bach 1910: pl. 10, fig. 5), and matches best with the M3 from Kornberg (Mottl 1969: pl. 12).

Overall, there exists evident metric and morphological variability within the *Tetralophodon* sample of Europe, while the uncertain stratigraphic position for some of them obscures whether this variability has taxonomic/biochronologic importance. Additionally, it should be noted that none of the above dental traits should be used on its own for any taxonomic/biochronologic conclusions (e.g., Obertiefenbach with 4–4 ½ lophs and Kornberg with five lophs have approximately similar age; Fig. 18) especially when studying limited/fragmentary samples. In this aspect, the secure chronological placement of the HAM 6 morphological traits allows their chronological control and can form a reliable comparative sample, contributing thus to the investigation of the evolution of European *Tetralophodon*.

Minimum number of individuals – age, sex, health, and hypotheses on the cause of death

Based on the degree of dental wear and the dental eruption sequence in deinotheres and elephantimorph proboscideans, we can calculate the Minimum Number of Individuals for each HAM layer. HAM 4 includes one juvenile *Deinotherium* individual; HAM 5 two juveniles (of which one partial skeleton is preserved) and one adult (based on tooth fragments) *Deinotherium* individuals, and two juveniles and one adolescent (based on the P3) *Tetralophodon* individuals; HAM 6 one (or perhaps two; see below) adult *Tetralophodon* individual (partial skeleton).

The *Deinotherium* mandible from HAM 5 belonged to an individual in its infancy (dp4 not fully erupted) in accordance with the developmental stage of the preserved postcranial bones. Although hypothetical, this very early age at death of the individual might be the result of predation. The damaged angles of the mandible might be attributed to carnivore gnawing, because this region (which includes the masseteric fossa where the masseter muscle is attached) is commonly attacked by carnivorans (Binford 1981: p. 63, fig. 3.27; Brain 1981: pp. 69–70, fig. 62). Interestingly, HAM 5 is the only layer of Hammerschmiede that documents both a machairodont felid (*Pseudaelurus*) and a large-sized hyaenid (Kargopoulos 2022; Kargopoulos et al. 2022), both formidable predators capable for foraging on juvenile proboscideans, which might have been inattentive or were possible left unprotected by the herd.

Applying the dental age classes of Metz-Muller (2000) (see Material and methods) in the HAM 6 *Tetralophodon* molars, the m2 (C, D, D/d, d) and M2 (D/d, D/d, d/p, f) correspond to an age class of ~ 10 (compatible with the severely worn M1, and the practically unworn m3 fragment), and the M3 (C, C, D, d, f) to ~ 13. The m2/M2 provide an ontogenetic age estimation ~ 25–36, and the M3 ~ 37–48, in *Loxodonta africana* equivalent years (Metz-Muller 2000: fig. 22). As noted in the taphonomic section, the excavation of fossils at HAM 6 took place in the end of 1970ies and early 1980ies, and therefore there are not precise spatial data available. The wear of the right m2 is roughly compatible (but slightly in a more advanced stage indicating a stronger right-side component in the food consumption) with the left M2. Unfortunately, the right M2 is not available, however, the right M3 is significantly more worn than the left M2, as well as than the right m2. This is not compatible with the normal wear pattern and dental succession known in elephantimorph proboscideans, in which the preceding tooth is more worn than the succeeding one. This means either the presence of two individuals at HAM 6, or of a single one (of about 35–40 years old) with anomalous/pathologic dental condition. Another interesting aspect is the marked difference in the wear along the M3, whose mesial half is severely affected by wear, whereas the distal one is minimally worn.

For the HAM 6 *Tetralophodon* individual(s) a sex determination is possible. The large size of the m2/M2, in particular compared with the Rudabánya and Dinotheriensande ones (Fig. 16), indicates a male individual; the LM3 might be a slight underestimate of the original unworn condition, but it also fits better with a male determination. In further agreement, the cross-sectional dimensions of the upper tusk are close to those of the Villavieja del Cerro upper tusk (associated with a much-worn M3), which is attributed to a male individual (Mazo and Jordá Pardo 1997; Larramendi 2016). The live shoulder height (including flesh) of the latter individual is estimated at ~ 3.45 m and its body mass at ~ 10 tons (Larramendi 2016). Comparable shoulder height and body mass estimations could also be considered for the HAM 6 individual(s).

Male proboscideans (documented also by their abundance in the fossil record of open-air sites where partial skeletons are preserved) show a high mortality at their subadult/adult (but not senile) stage, which is possibly attributed to the fact that males on puberty are forced out of the family and acquire a more solitary and nomadic life associated with increased risks (Konidaris and Tourloukis 2021, and references cited therein). Whether one or two individuals at HAM 6, the dental wear evidence indicates an adulthood stage, certainly younger than the expected longevity, and therefore a comparable way of life can be hypothesized also for the HAM 6 *Tetralophodon*. Additionally,

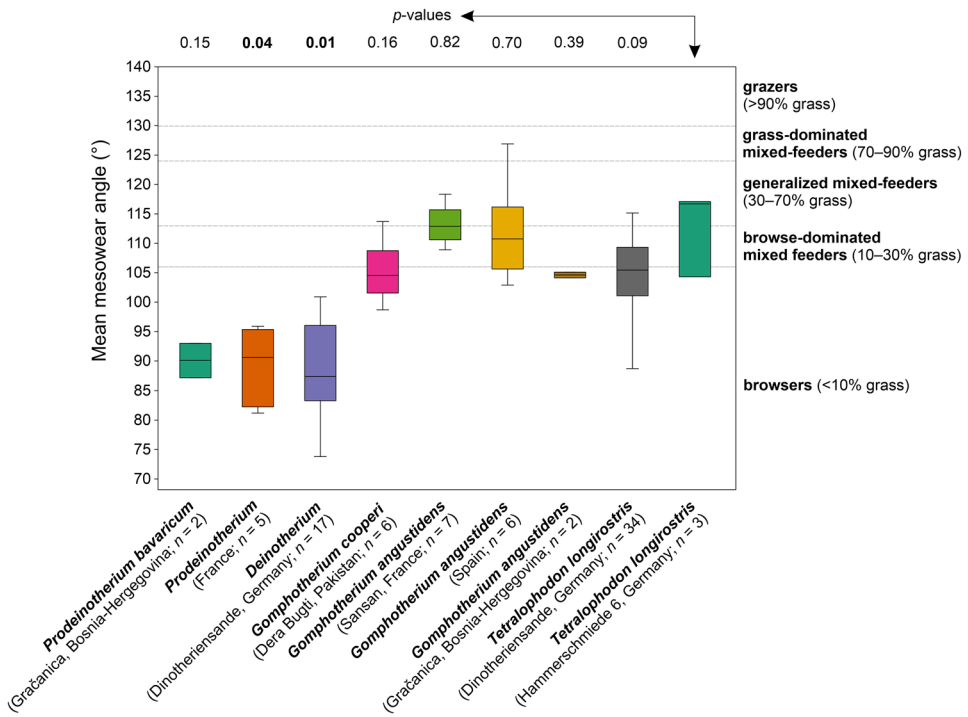

Fig. 17 Box-and-whisker plots comparing the dental mesowear angles of *Tetralophodon longirostris* from Hammerschmiede with various Miocene proboscideans. Estimated dietary composition and categories are indicated with dashed lines based on Saarinen et al. (2015); comparative data from Xafis et al. (2020). The *p*-values above the graph were calculated by pairwise Mann–Whitney test comparing the mesowear angles of *Tetralophodon longirostris* from Hammerschmiede with the other proboscideans; significant differences at $p < 0.05$ are bolded

the HAM 6 molars exhibit some enamel hypoplasia (e.g., Fig. 15b–c), indicating episodes of stress (physiological, ecological, predatory, or competitive) during the life history (see e.g., Ameen et al. 2020), which may have rendered the individual(s) weakened, and potentially could have also contributed to a premature death (based on the available tooth positions and the degree of dental wear).

Dental mesowear analysis and palaeoecological remarks

The mean mesowear angles of the three *Tetralophodon longirostris* molars from HAM range from ~ 104° to ~ 117° (Table 6), thus showing moderately angled wear facets and modestly deep worn dentine valleys. This provides a mixed-feeding mesowear signal with an important browsing component (Fig. 17). The mean mesowear angles from HAM are significantly different from the heavily browse-dominated diet of *Prodeinotherium* (Gračanica and France) and *Deinotherium* (Dinotheriensande), supported also by the low *p*-values from the pairwise Mann–Whitney test (Fig. 17). On the other hand, the HAM signal fits within the variable range of *Gomphotherium* spp. and *Tetralophodon longirostris* (Dinotheriensande), which broadly show a browsing to mixed feeding diet. The mean value (112.7°) plots the HAM *Tetralophodon* within the browse-dominated mixed feeding category and closer to the Middle Miocene *G. angustidens* populations from Sansan (France; mean value 113.5°) and Spain (mean value 111.7°), supported also by the *p*-values. However, the median value (116.7°) of the HAM 6 T. *longirostris* exceeds those of all comparative samples, while its upper range exceeds the upper quartile of both *G. angustidens* populations, implying perhaps a slightly higher incorporation of grasses in the diet. Interestingly, the HAM 6 T. *longirostris* shows a more expressed generalized mixed-feeding signal than the *T. longirostris* population from Dinotheriensande, which could perhaps reflect slightly different palaeoenvironmental conditions. We note, however, that the Dinotheriensande material lacks stratigraphic control and may be mixed, encompassing a long biostratigraphic range, that may cover both Astaracian and Vallesian. Additionally, the HAM sample is limited, and therefore the results should be considered indicative but not conclusive. Although mesowear angles were not acquired for the HAM deinotheres, several studies support the browsing character and the consumption of C_3 vegetation of *D. levius* / *D. giganteum* populations from the Middle–Late Miocene of central Europe (Calandra et al. 2008; Aiglstorfer et al. 2014b; Xafis et al. 2020). As such, the different feeding habits of *D. levius* and *T. longirostris* indicate niche partitioning between these two species, i.e., they did not compete for the same food resources, thus reducing the competitive pressure and permitting their viable coexistence at Hammerschmiede.

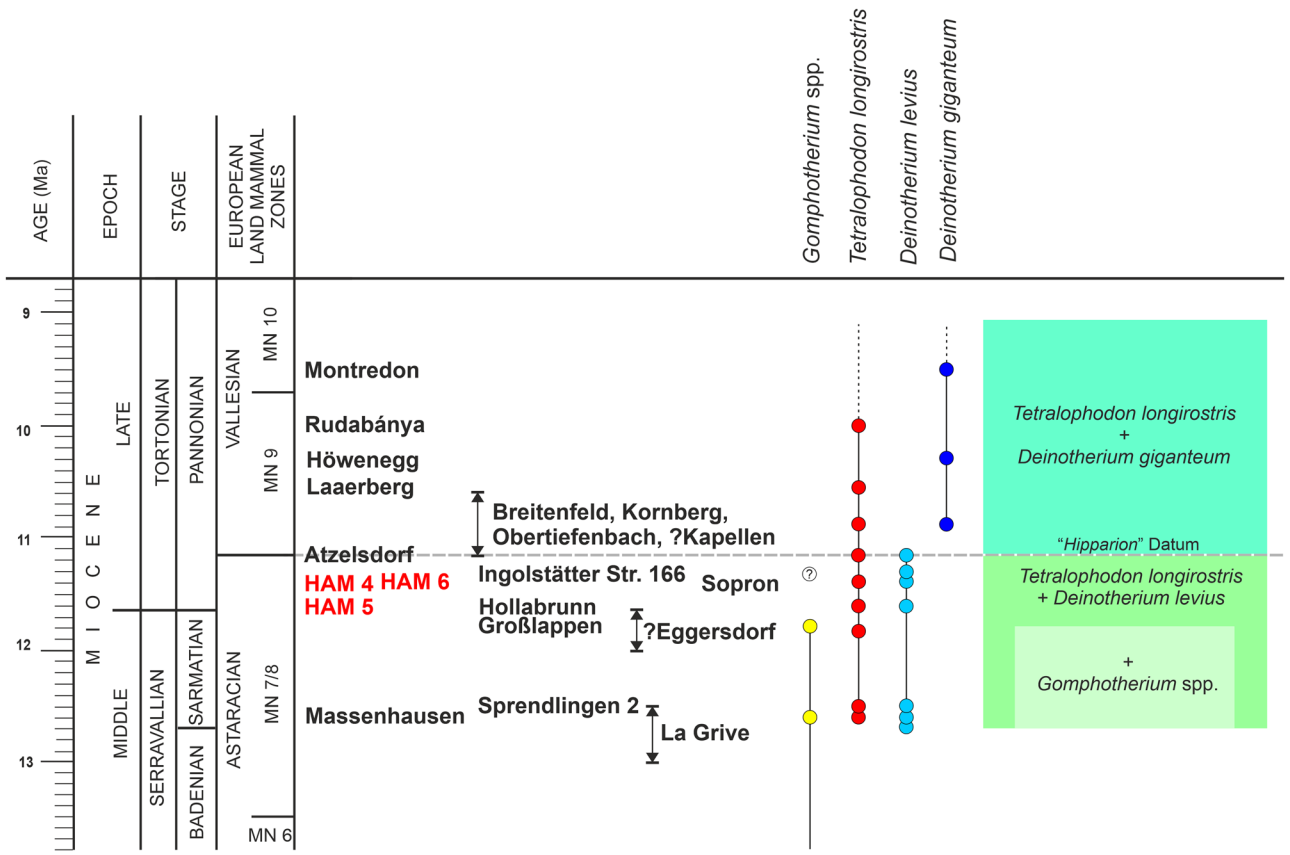

Fig. 18 Biochronological distribution of *Deinotherium levius*, *Deinotherium giganteum*, *Gomphotherium* spp. and *Tetralophodon longirostris* close to the Middle–Late Miocene transition, and chronology of selected central European localities. Data from Göhlich (1998), Böhme et al. (2012) and Kirscher et al. (2016)

Biostratigraphic remarks – conclusions

The proboscidean sample from Hammerschmiede includes complete and important specimens of the deinotheriid *Deinotherium levius* and the gomphotheriid *Tetralophodon longirostris*. Besides its taxonomic value, the securely bio- and magnetostratigraphically constrained age of the HAM localities (Kirscher et al. 2016), renders the HAM proboscidean assemblage important for biostratigraphic conclusions within the wider central European context, close to the Middle/Late Miocene transition (Fig. 18).

Evidence of association of *D. levius* and *T. longirostris* is so far relatively meager and besides Hammerschmiede, these species coexisted at the late Middle Miocene (MN 7/8) localities Massenhausen (Gräf 1957; Göhlich 1998), Sprendlingen 2 (Germany; Böhme et al. 2012) and Montréjeau (France; Crouzel 1947; Crouzel and Debeaux 1957; Duranthon et al. 2007), and the early Late Miocene localities Atzelsdorf (earliest MN 9; Göhlich and Huttunen 2009, see also Konidaris and Koufos 2019) and Polinya (MN 9; Alberdi 1971; Casanovas-Vilar et al. 2016). Both species are recorded at Dinotheriensande (e.g., p3 of *D. levius* from Eppelsheim HLMD-Din 311), but the absence of stratigraphic data and the reworking of the fossils (Böhme et al. 2012; Pickford and Pourabrishami 2013) makes their cooccurrence only hypothetical. Another locality with possible such coexistence is Hollabrunn (formerly Oberhollabrunn; Austria), from where Sickenberg (1928, 1929) mentions *Deinotherium* sp. and *Mastodon* sp. A deinothere P3 from Hollabrunn is attributed to *D.* aff. *giganteum* by Thenius (1952: p. 133, table), who notes (p. 132) that such an attribution corresponds to a form between *D. levius* and *D. giganteum*. Indeed, the dimensions of the tooth plot at the lower values of *D. giganteum* from Montredon (MN 10, France; Tobien 1988; Ginsburg and Chevrier 2001), but also within *D. levius* from Massenhausen, Hinterauerbach (Germany; Gräf 1957) and Gusyatin (Ukraine; Svistun 1974). Additionally, a DP3 from Hollabrunn is attributed to *D. giganteum* by Huttunen (2002a, b; the author followed the two European deinothere species concept of *Prodeinotherium bavaricum-Deinotherium giganteum*), but the tooth is smaller than the few known specimens of *D. giganteum*, and interestingly has close dimensions to the corresponding one from HAM, especially in terms of length (Fig. 7). The preserved cheek tooth of *Mastodon* sp. from

Hollabrunn (Sickenberg 1929) is much worn and does not provide any taxonomic information, however, a distal fragment of a M3 from "Schottergrube in Haslach am Reisberg bei Oberhollabrunn" is attributed by Schlesinger (1917: p. 101, pl. 17, fig. 1) to *Tetralophodon longirostris*. Importantly, the overall large mammal faunas from Hollabrunn and HAM have almost half of the taxa in common and are regarded roughly contemporaneous by Kirscher et al. (2016). The latter authors note faunal similarities also between HAM and Ingolstädter Straße 166 of Munich city (likewise in the central North Alpine Foreland Basin in Bavaria, Germany). From this site Stromer (1938) described a partial deinothere skeleton and attributes it to *D. giganteum*, noting its small dental dimensions; later on, Gräf (1957: p. 144) places this find in the synonymy list of *D. levius*. Stromer (1338: p. 26, 1940: p. 60, pl. 3, fig. 13) described two m3 distal fragments of a gomphothere, ascribing them to cf. *Trilophodon angustidens* var. *subtapiroidea*, which later on Göhlich (1998: p. 67) attributes them to *G.* cf. *steinheimense*. Both authors note the difficulty in the identification of these fragments and the possibility that they could instead belong to *Tetralophodon*. Therefore, the presence of *Gomphotherium* at Ingolstädter Straße 166 is considered tentative.

Although the absence of a faunal element in a fossil assemblage (especially in the smaller ones and in particular concerning the rarer proboscideans) cannot be regarded as evidence of its nonexistence, the presence of *Gomphotherium* (together with *Tetralophodon*) at Massenhausen, and its absence to date at HAM (as well as at Atzelsdorf and other contemporaneous sites; *Gomphotherium* in the Eppelsheim Formation originates most probably from pre-Late Miocene deposits; see Göhlich 2020) may indicate a younger character for the HAM proboscidean fauna (Fig. 18). Hammerschmiede is either correlated after the extinction of *Gomphotherium* or at least to the period that captures its decline, which roughly coincides with the appearance of tetralophodont gomphotheres. Therefore, HAM (beginning of Tortonian; earliest Late Miocene) showcases the transition from the Middle Miocene trilophodont (*Gomphotherium*)-dominated faunas of central Europe (with Massenhausen and Großlappen, Germany, documenting some of the *Gomphotherium* last occurrences, and one of the first ones of *Tetralophodon* at the former) to the Late Miocene tetralophodont-dominated ones (*Tetralophodon*, and later on *Konobelodon* and *Anancus*). It seems thus possible that *Gomphotherium* did not manage to enter into the Late Miocene and possibly vanished close to the Seravallian/Tortonian boundary, when tetralophodonts seem to have been the major elephantimorph component. Therefore, the association *D. levius* and *T. longirostris* covers the Sarmatian and the base of Pannonian (Tortonian), while their association with *Gomphotherium* spp. correlates to the Sarmatian, and thus can be regarded as a useful biochronologic tool for the central Europe terrestrial settings (Fig. 18). The demise and extinction of trilophodont gomphotheres could potentially be linked to the climatic changes that occurred during this epoch (see e.g., Böhme et al. 2008) as well as to the competition with the tetralophodont ones (see e.g., their broadly similar dental mesowear signal), or both. Whether tetralophodont gomphotheres contributed to the extinction of trilophodont gomphotheres through direct competition for resources or filled the gap left by the decline and extinction of the latter is difficult to prove, and beyond the scope of this study. However, it emphasizes the need for further and systematic research into this topic, and proboscidean material from localities correlated to this time interval such as HAM, as well as the discovery of new ones from controlled stratigraphic contexts, is crucial.

Supplementary information The online version contains supplementary material available at https://doi.org/10.1007/s10914-023-09683-3.

Acknowledgements The authors would like to express their special thanks to the two private collectors †S. Guggenmos (Dösingen) and M. Schmid (Marktoberdorf) for the great cooperation and the transfer and making available of their finds and records. Further, we wish to thank C. Kyriakouli and A.-C. Grupp for the preparation of the partial skeleton of the juvenile deinothere (both at that time at SNSB) and H. Stöhr (GPIT) for the preparation of the other specimens. We thank A. Fatz (Tübingen) for providing photographs of the fossil material, and G. Ferreira and C. Kyriakouli (both Tübingen) for realizing the µCT scanning. We acknowledge all participants of the numerous excavations in the Hammerschmiede fossil site since 2011, who helped to detect and collect the studied material. Since 2020, the excavations and associated research were supported by the Bavarian State Ministry of Research and the Arts, and by the Bavarian Natural History Collections (SNSB). GK would like to thank for granting access to collections at their disposal: O. Sandrock (HLMD), G. Rössner (SNSB-BSPG), U. Göhlich (NHMW), P. Tassy (MNHN), M. Gasparik (HNHM), L. Kordos (HGI), D. Berthet (ML), A. Prieur (FSL), and I. Werneburg (GPIT). G.K. was supported by the European Union-funded Integrated Activities grant SYNTHESYS (AT-TAF-3825 and HU-TAF-1683), and DFG-463225251 ("MEGALOPOLIS"). We thank the editor D. Croft, and the reviewers J. Saarinen and one anonymous, for their constructive comments and suggestions.

Authors' contributions Conceptualization: G.K., M.B. Formal analysis: G.K. Investigation: G.K., T.L., P.K., M.B. Methodology: G.K. Project administration: M.B. Validation: G.K., M.B. Visualization: G.K., T.L., M.B. Writing – original draft: G.K., T.L., M.B. Writing – review and editing: G.K., T.L., P.K., M.B.

Funding Open Access funding enabled and organized by Projekt DEAL.

Availability of data and materials All data are included in this published article and its supplementary information files.

Declarations

Competing interests The authors have no competing interests to declare that are relevant to the content of this article.

References

Abràmoff MD, Magalhães, PJ, Ram SJ (2004) Image processing with ImageJ. Biophotonics Int 11:36–42.

Alba DM, Gasamans N, Pons-Monjo G, Luján ÀH, Robles JM, Obradó P, Casanovas-Vilar I (2020) Oldest *Deinotherium proavum* from Europe. J Vertebr Paleontol 40:e1775624.

Álvarez-Lao DJ, Méndez M (2011) Ontogenetic changes and sexual dimorphism in the mandible of adult woolly mammoths (*Mammuthus primigenius*). Geobios 44:335–343.

Aiglstorfer M, Göhlich UB, Böhme M, Gross M (2014a) A partial skeleton of *Deinotherium* (Proboscidea, Mammalia) from the late Middle Miocene Gratkorn locality (Austria). Palaeobiodivers Palaeoenviron 94:49–70.

Aiglstorfer M, Bocherens H, Böhme, M (2014b) Large mammal ecology in the late Middle Miocene Gratkorn locality (Austria). Palaeobiodivers Palaeoenviron 94:189–213.

Alberdi MT (1971) Primer ejemplar completo de un *Tetralophodon longirostris* Kaup, 1835, encontrado en España. Estud Geol 27:181–196.

Ameen M, Khan A, Tahir Waseem M, Ahmad R, Iqbal A, Rafeh A, Imran M (2020) Were late gomphotheres (Plio-Pleistocene) of the Siwaliks at more stress as compared to early gomphotheres (middle to late Miocene)? J Bioresour Manag 7:117–130.

Antunes MT, Mazo AV (1983) Quelques mastodontes Miocènes du Portugal. Ciênc Terra 7:115–128.

Arambourg C (1934) Le *Dinotherium* des gisements de l'Omo. C R Soc Géol Fr 1934:86–87.

Bach F (1910) Mastodonreste aus der Steiermark. Beitr Paläont Geol Öster-Ung und des Orients 23:63–123.

Bakalov P, Nikolov I (1962) Les Fossiles de Bulgarie. X. Mammifères Tertiaires. Académie des Sciences de Bulgarie, Sofia.

Bakalow P (1914) Beiträge zur Paläontologie Bulgariens. II. Dinotheriumreste aus Bulgarien. Ann Univ Sofia 8–9:1–29.

Behrensmeyer AK (1975) The taphonomy and paleoecology of Plio-Pleistocene vertebrate assemblages east of Lake Rudolf, Kenya. Bull Mus Comp Zool 146:473–578.

Bergounioux FM, Crouzel F (1960) *Tetralophodon curvirostris* n. sp. (Mamm., Proboscidea) aus dem Unterpliozän (Pontien) von Esselborn (Rheinhessen). Jahresber Mitt Oberrhein Geol Ver 42:109–121.

Binford LR (1981) Bones: Ancient Men and Modern Myths. Academic Press, New York.

Böhme M, Ilg A, Winklhofer M (2008) Late Miocene "washhouse" climate in Europe. Earth Planet Sci Lett 275:393–401.

Böhme M, Aiglstorfer M, Uhl D, Kullmer O (2012) The antiquity of the Rhine River: Stratigraphic coverage of the Dinotheriensande (Eppelsheim Formation) of the Mainz Basin (Germany). PLoS One 7:e36817.

Böhme M, Spassov N, Fuss J, Tröscher A, Deane AS, Prieto J, Kirscher U, Lechner T, Begun DR (2019) A new Miocene ape and locomotion in the ancestor of great apes and humans. Nature 575:489–493.

Böhme M, Spassov N, DeSilva JM, Begun DR (2020) Reply to: Reevaluating bipedalism in *Danuvius*. Nature 586: E4–E5.

Bonaparte CL (1845) Catalogo Metodico dei Mammiferi Europei. Luigi di Giacomo Pirola, Milan.

Brain CK (1981) The Hunters or the Hunted? An Introduction to African Cave Taphonomy. The University of Chicago Press, Chicago and London.

Calandra I, Göhlich UB, Merceron G (2008) How could sympatric megaherbivores coexist? Example of niche partitioning within a proboscidean community from the Miocene of Europe. Naturwissenschaften 95:831–838.

Casanovas-Vilar I, Madern A, Alba DM, Cabrera L, García-Paredes I, van den Hoek Ostende LW, DeMiguel D, Robles JM, Furió M, van Dam JA, Garcés M, Angelone C, Moyà-Solà S (2016) The Miocene mammal record of the Vallès-Penedès Basin (Catalonia). C R Palevol 15:791–812.

Crouzel F (1947) Une variété de *Dinotherium levius* dans le Miocène de Montréjeau. Bull Soc hist nat Toulouse 82:105–109.

Crouzel F, Debeaux M (1957) Découverte de *Tetralophodon longirostris* près de Montréjeau (Haute-Garonne). Bull Soc hist nat Toulouse 92:202–204.

Cuvier G (1817) Le Règne Animal. Déterville, Paris.

Delmer C (2009) Reassessment of the generic attribution of *Numidotherium savagei* and the homologies of lower incisors in proboscideans. Acta Palaeontol Pol 54:561–580.

Depéret C (1887) Recherches sur la succession des faunes de vertébrés miocènes de la vallée du Rhône. Arch Mus hist nat Lyon 4:45–313.

Doppler G (1989) Zur Stratigraphie der nördlichen Vorlandmolasse in Bayerisch-Schwaben. Geol Bavar 94:83–133.

Duranthon F, Antoine PO, Laffont D, Bilotte M (2007) Contemporanéité de *Prodeinotherium* et *Deinotherium* (Mammalia, Proboscidea) à Castelnau-Magnoac (Hautes-Pyrénées, France). Rev Paléobiol 26:403–411.

Eichwald E (1831) Zoologia Specialis Quam Expositis Animalibus Tum Vivis, Tum Fossilibus Potissimum Rossiae in Universum, et Poloniae in Specie. Josephi Zawadzki, Vilnae.

Falconer H (1857) On the species of mastodon and elephant occurring in the fossil state in Great Britain. Part I. *Mastodon*. Q J Geol Soc Lond 13:307–360.

Ferretti MP, Rook L, Torre D (2003) *Stegotetrabelodon* (Proboscidea, Elephantidae) from the Late Miocene of southern Italy. J Vertebr Paleontol 23:659–666.

Fuss J, Prieto J, Böhme M (2015) Revision of the boselaphin bovid Miotragocerus monacensis Stromer, 1928 (Mammalia, Bovidae) at the Middle to Late Miocene transition in Central Europe. N Jb Min Geol Paläont – Abh 276:229–265.

Gagliardi F, Maridet O, Becker D (2021) The record of Deinotheriidae from the Miocene of the Swiss Jura Mountains (Jura Canton, Switzerland). bioRxiv 244061, ver. 4 peer-reviewed by PCI Paleo, 2020.2008.2010.244061.

Garevski R, Markov GN (2011) A *Deinotherium gigantissimum* (Mammalia, Proboscidea) palate with deciduous dentition from the area of Veles, Republic of Macedonia. Paläont Z 85:33–36.

Gasparik M (2004) Magyarországi Neogén és Also-Pleisztocén Proboscidea Maradványok. Dissertation, Magyar Természettudományi Múzeum, Budapest.

Gasparik M (2005) Proboscidean remains from the Pannonian of Rudabánya. Palaeontogr Ital 90:181–192.

Gaziry AW (1976) Jungtertiäre Mastodonten aus Anatolien (Türkei). Geol Jb 22:3–143.

Gaziry AW (1994) Über Mastodonten (Mammalia. Proboscidea) aus den Dinotheriensanden (M-Europa: Ober-Miozän): Materialien des Hessischen Landesmuseums Darmstadt. Verh naturwiss Ver Hamburg 34:95–112.

Gaziry AW (1997) Die Mastodonten (Proboscidea, Mammalia) aus Dorn-Dürkheim 1 (Rheinhessen). Cour Forsch-Inst Senckenberg 197:73–115.

Geraads D, Kaya T, Mayda S (2005) Late Miocene large mammals from Yulaflı, Thrace region, Turkey, and their biogeographic implications. Acta Palaeontol Pol 50:523–544.

Ginsburg L, Chevrier F (2001) Les Dinothères du bassin de la Loire et l'évolution du genre *Deinotherium* en France. Symbioses 5:9–24.

Göhlich UB (1998) Elephantoidea (Proboscidea, Mammalia) aus dem Mittel- und Obermiozän der Oberen Süßwassermolasse Süddeutschlands: Odontologie und Osteologie. Münchner Geowiss Abh A Geol Paläont 36:1–245.

Göhlich UB (1999) Order Proboscidea. In: Rössner GE, Heissig K (eds) The Miocene Land Mammals of Europe. Dr. Friedrich Pfeil, Munich, pp 157–168.

Göhlich UB (2010) The Proboscidea (Mammalia) from the Miocene of Sandelzhausen (southern Germany). Paläont Z 84:163–204.

Göhlich UB (2020) The proboscidean fauna (Mammalia) from the middle Miocene lignites of Gračanica near Bugojno (Bosnia–Herzegovina). Palaeobiodivers Palaeoenviron 100:413–436.

Göhlich UB, Huttunen K (2009) The early Vallesian vertebrates of Atzelsdorf (Late Miocene, Austria) 12. Proboscidea. Ann Naturhist Mus Wien 111A:635–646.

Gräf IE (1957) Die Prinzipien der Artbestimmung bei *Dinotherium*. Palaeontographica 108:131–185.

Hammer Ø, Harper DAT, Ryan PD (2001) PAST: paleontological statistics software package for education and data analysis. Palaeontol Electron 4:1–9.

Harris JM (1976) Cranial and dental remains of *Deinotherium bozasi* (Mammalia: Proboscidea) from East Rudolf, Kenya. Zool J Linn Soc 178:57–75.

Harris JM (1983) Deinotheriidae. In: Harris JM (ed) Koobi Fora Research Project, Volume 2: The Fossil Ungulates: Proboscidea, Perissodactyla, and Suidae. Clarendon Press, Oxford, pp 22–39.

Hartung J, Böhme M (2022) Unexpected cranial sexual dimorphism in the tragulid *Dorcatherium naui* based on cranial material from the middle to late Miocene localities of Eppelsheim and Hammerschmiede (Germany). PLoS ONE 17: e0267951.

Hartung J, Lechner T, Böhme M (2020) New cranial material of *Miotragocerus monacensis* (Mammalia: Bovidae) from the late Miocene hominid locality Hammerschmiede (Germany). Neues Jahrb Geol Paläontol - Abh 298:269–284.

Hautier L, Mackaye HT, Lihoreau F, Tassy P, Vignaud P, Brunet M (2009) New material of *Anancus kenyensis* (Proboscidea, Mammalia) from Toros-Menalla (Late Miocene, Chad): Contribution to the systematics of African anancines. J African Earth Sci 53:171–176.

Hay OP (1922) Further observations on some extinct elephants. Proc Biol Soc Wash 35:97–101.

Haynes G (1988) Longitudinal studies of African elephant death and bone deposits. J Achaeol Sci 15:131–157.

Haynes G. (1991) Mammoths, Mastodonts and Elephants: Biology, Behavior, and the Fossil Record. Cambridge University Press, Cambridge.

Huttunen K (2002a) Systematics and taxonomy of the European Deinotheriidae (Proboscidea, Mammalia). Ann Naturhist Mus Wien 103A:237–250.

Huttunen K (2002b) Deinotheriidae (Proboscidea, Mammalia) dental remains from the Miocene of Lower Austria and Burgenland. Ann Naturhist Mus Wien 103A:251–285.

Huttunen K, Göhlich UB (2002) A partial skeleton of *Prodeinotherium bavaricum* (Proboscidea, Mammalia) from the Middle Miocene of Unterzolling (Upper Freshwater Molasse, Germany). Geobios 35:489–514.

Illiger C (1811) Prodromus Systematis Mammalium et Avium Additis Terminis Zoographicis Utriusque Classis. C. Salfield, Berlin.

Jourdan M (1861) Des terrains sidérolitiques. C R Hebd Séances Acad Sci 53:1009–1014.

Kargopoulos N (2022) The carnivorans (Carnivora, Mammalia) from the hominid locality of Hammerschmiede (Bavaria, Germany). Dissertation, University of Tübingen, Tübingen.

Kargopoulos N, Kampouridis P, Lechner T, Böhme M (2021a) A review of *Semigenetta* (Viverridae, Carnivora) from the Miocene of Eurasia based on material from the hominid locality of Hammerschmiede (Germany). Geobios 69:25–36.

Kargopoulos N, Kampouridis P, Lechner T, Böhme M (2021b) Hyaenidae (Carnivora) from the Late Miocene hominid locality of Hammerschmiede (Bavaria, Germany). Hist Biol 34:2249–2258.

Kargopoulos N, Valenciano A, Abella J, Kampouridis P, Lechner T, Böhme M (2022) The exceptionally high diversity of small carnivorans from the Late Miocene hominid locality of Hammerschmiede (Bavaria, Germany). PLoS ONE 17: e0268968.

Kargopoulos N, Valenciano A, Kampouridis P, Lechner T, Böhme M (2021c) New early late Miocene species of *Vishnuonyx* (Carnivora, Lutrinae) from the hominid locality of Hammerschmiede, Bavaria, Germany. J Vertebr Paleontol 41:e1948858.

Kaup J (1829) *Deinotherium giganteum*. Eine Gattung der Vorwelt aus der Ordnung der Pachydermen. Isis 22:401–404.

Kaup JJ (1832a) Description d'Ossements Fossiles de Mammifères Inconnus Jusqu'à Présent, qui se Trouvent au Muséum Grandducal de Darmstadt. J.G. Heyer, Darmstadt.

Kaup J (1832b) Ueber zwei Fragmente eines Unterkiefers von *Mastodon angustidens* Cuv., nach welchen diese Art in die Gattung *Tetracaulodon* Godmann gehört. Isis 25:628–631.

Kaup JJ (1835) Description d'Ossements Fossiles de Mammifères Inconnus Jusqu'à-Présent qui se Trouvent au Muséum Grandducal de Darmstadt. Diehl, J.P., Darmstadt, pp 65–89.

Kaup JJ, Scholl JB (1864) Verzeichnis der Gypsabgüsse von den ausgezeichnetsten urweltlichen Thierresten des Großherzoglichen Museums zu Darmstadt, Darmstadt.

Khomenko J (1914) La faune méotique du village Taraklia du district de Bendery. Trudy Bessarab Obsh Est liub est 5:1–55

Kirscher U, Prieto J, Bachtadse V, Abdul Aziz H, Doppler G, Hagmaier M, Böhme M (2016) A biochronologic tie-point for the base of the Tortonian stage in European terrestrial settings: Magnetostratigraphy of the topmost Upper Freshwater Molasse sediments of the North Alpine Foreland Basin in Bavaria (Germany). Newsl Stratigr 49:445–467.

Klähn H (1922) Die badischen Mastodonten und ihre süddeutschen Verwandten. Verlag von Gebrüder Borntraeger, Berlin.

Klähn H (1931) Rheinhessisches Pliozän besonders Unterpliozän im Rahmen des Mitteleuropäischen Pliozäns. Geol Paläont Abh 18:279–340.

Konidaris GE, Koufos GD (2016) Palaeontology of the upper Miocene vertebrate localities of Nikiti (Chalkidiki Peninsula, Macedonia, Greece). Proboscidea. Geobios 49:37–44.

Konidaris GE, Koufos G (2019) Late Miocene proboscideans from Samos Island (Greece) revisited: new specimens from old collections. Paläont Z 93:115–134.

Konidaris GE, Roussiakis SJ (2019) The first record of *Anancus* (Mammalia, Proboscidea) in the late Miocene of Greece and reappraisal of the primitive anancines from Europe. J Vertebr Paleontol 38:e1534118.

Konidaris GE, Tsoukala E (2020) Proboscideans from the upper Miocene localities of Thermopigi, Neokaisareia and Platania (Northern Greece). Ann Paléontol 106:102380.

Konidaris GE, Tsoukala E (2022) The fossil record of the Neogene Proboscidea (Mammalia) in Greece. In: Vlachos E (ed) The Fossil Vertebrates of Greece Vol. 1. Springer – Nature Publishing Group, Cham, pp 299–344.

Konidaris GE, Tourloukis V (2021) Proboscidea-*Homo* interactions in open-air localities during the Early and Middle Pleistocene of

western Eurasia: a palaeontological and archaeological perspective. In: Konidaris GE, Barkai R, Tourloukis V, Harvati K (eds) Human-Elephant Interactions: From Past to Present. Tübingen University Press, Tübingen, pp 67–104.

Konidaris GE, Roussiakis SJ, Theodorou GE, Koufos GD (2014) The Eurasian occurrence of the shovel-tusker *Konobelodon* (Mammalia, Proboscidea) as illuminated by its presence in the late Miocene of Pikermi (Greece). J Vertebr Paleontol 34:1437–1453.

Konidaris GE, Roussiakis SJ, Athanassiou A, Theodorou GE (2017) The huge-sized deinothere *Deinotherium proavum* (Proboscidea, Mammalia) from the Late Miocene localities Pikermi and Halmyropotamos (Greece). Quat Int 430:5–21.

Kovachev D (2004) Cranium of *Stegotetrabelodon* (Proboscideo, Mammalia) from the Neogene in the East Maritsa basin. Rev Bulg Geol Soc 65:167–173.

Larramendi A (2016) Shoulder height, body mass, and shape of proboscideans. Acta Palaeontol Pol 61:537–574.

Lartet E (1859) Sur la dentition des proboscidiens fossiles (*Dinotherium*, mastodontes et éléphants) et sur la distribution géographique et stratigraphique de leurs débris en Europe. Bull Soc Géol Fr 16:469–515.

Lechner T, Böhme M (2022) The beaver *Steneofiber depereti* from the lower Upper Miocene hominid locality Hammerschmiede and remarks on its ecology. Acta Palaeontol Pol 67: 807–826.

Lechner T, Böhme M (2023) The largest record of the minute beaver *Euroxenomys minutus* (Mammalia, Castoridae) from the early Late Miocene hominid locality Hammerschmiede (Bavaria, Southern Germany) and palaeoecological considerations. Hist Biol. https://doi.org/10.1080/08912963.2023.2215236

Linnaeus C (1758) Systema Naturae per Regna Tria Naturae, Secundum Classes, Ordines, Genera, Species, cum Characteribus, Differentiis, Synonymis Locis. Tomus 1. Laurentius Salvius, Stockholm.

Mayr G, Lechner T, Böhme M (2020a) A skull of a very large crane from the late Miocene of Southern Germany, with notes on the phylogenetic interrelationships of extant Gruinae. J Ornithol 161:923–933.

Mayr G, Lechner T, Böhme M (2020b) The large-sized darter *Anhinga pannonica* (Aves, Anhingidae) from the late Miocene hominid Hammerschmiede locality in Southern Germany. PLoS ONE 15:e0232179.

Mayr G, Lechner T, Böhme M (2022) Nearly complete leg of an unusual, shelduck-sized anseriform bird from the earliest late Miocene hominid locality Hammerschmiede (Germany). Hist Biol 35:465–474.

Mayr H, Fahlbusch (1975). Eine unterpliozäne Kleinsäugerfauna aus der Oberen Süßwasser-Molasse Bayerns. Mitt Bayer Staatssamml Paläontol Hist Geol 15:91–111.

Mazo AV, Montoya P (2003) Proboscidea (Mammalia) from the Upper Miocene of Crevillente (Alicante, Spain). Scr Geol 126:79–109.

Mazo AV, van der Made J (2012) Iberian mastodonts: Geographic and stratigraphic distribution. Quat Int 255:239–256.

Mazo AV, Jordá Pardo JF (1997) Un *Tetralophodon longirostris* (Kaup, 1832) (Proboscidea, Mammalia) en el Mioceno medio de Villavieja del Cerro (sector central de la cuenca del Duero, Valladolid). Rev Soc Geol Esp 10:219–235.

Metz-Muller F (1995) Mise en évidence d'une variation intraspécifique des caractères dentaires chez *Anancus arvernensis* (Proboscidea, Mammalia) du gisement de Dorkovo (Pliocène ancien de Bulgarie, biozone MN14). Geobios 28:737–743.

Metz-Muller F (2000) La population d'*Anancus arvernensis* (Proboscidea, Mammalia) du Pliocène de Dorkovo (Bulgarie); étude des modalités évolutives d'*Anancus arvernensis* et phylogénie du genre *Anancus*. Dissertation, Muséum National d'Histoire Naturelle, Paris.

Mottl M (1969) Bedeutende Proboscidier-Neufunde aus dem Altpliozän (Pannonien) Südost-Österreichs. Österreichische Akademie der Wissenschaften. Mathematisch-naturwissenschaftliche Klasse. Denkschriften 115:1–50.

Osborn HF (1921) The evolution, phylogeny, and classification of the Proboscidea. Am Mus Novit 1:1–15.

Osborn HF (1936) Proboscidea. A Monograph of the Discovery, Evolution, Migration and Extinction of the Mastodonts and Elephants of the World, Volume I: Moeritherioidea, Deinotherioidea, Mastodontoidea. American Museum Press, New York.

Pickford M, Pourabrishami Z (2013) Deciphering Dinotheriensande deinotheriid diversity. Palaeobiodivers Palaeoenviron 93:121–150.

Prieto J (2012) The genus *Eomyops* Engesser, 1979 (Rodentia, Eomyidae) from the youngest deposits of the German part of the North Alpine Foreland Basin. Swiss J Palaeontol 131:95–106.

Prieto J, Rummel M (2009) Evolution of the genus *Collimys* Daxner-Höck, 1972 (Rodentia, Cricetidae) a key to Middle to Late Miocene biostratigraphy in Central Europe. Neues Jahrb Geol Paläontol Abh 252:237–247.

Prieto J, van Dam JA (2012) Primitive Anourosoricini and Allosoricinae from the Miocene of Germany. Geobios 45:581–589.

Prieto J, van den Hoek Ostende LW, Böhme M, Braze M (2011) Reappearance of *Galerix* (Erinaceomorpha, Mammalia) at the Middle to Late Miocene transition in South Germany: biostratigraphic and palaeoecologic implications. Contrib Zool 80:179–189.

Saarinen J, Lister AM (2016) Dental mesowear reflects local vegetation and niche separation in Pleistocene proboscideans from Britain. J Quat Sci 31:799–808.

Saarinen J, Karme A, Cerling TE, Uno K, Säilä L, Kasiki S, Ngene S, Obari T, Mbua E, Manthi FK, Fortelius M (2015) A new tooth wear-based dietary analysis method for Proboscidea (Mammalia). J Vertebr Paleontol 35:e918546.

Sach VJ, Heizmann EPJ (2001) Stratigraphie und Säugetierfaunen der Brackwassermolasse in der Umgebung von Ulm (Südwestdeutschland). Stuttgarter Beiträge zur Naturkunde, Serie B (Geologie und Paläontologie) 310:1–95.

Sanders WJ (2003) Proboscidea. In: Fortelius M, Kappelman J, Sen S, Bernor RL (eds) Geology and Paleontology of the Miocene Sinap Formation, Turkey. Columbia University Press, New York, pp 202–219.

Schlesinger G (1917) Die Mastodonten des K. K. Naturhistorischen Hofmuseums. Denkschr K K Nat Hofmus 1:1–230.

Shoshani J, Tassy P (1996) Summary, conclusions, and a glimpse into the future. In: Shoshani J, Tassy P (eds) The Proboscidea: Evolution and Palaeoecology of Elephants and their Relatives. Oxford University Press, New York, pp 335–348.

Shoshani J, Golenberg EM, Yang H (1998) Elephantidae phylogeny: morphological versus molecular results. Acta Theriol Suppl 5:89–122.

Sickenberg O (1928) Säugetierreste aus der Umgebung von Oberhollabrunn. Verhandl Geol Bundesanst Wien 9–10:205–210.

Sickenberg O (1929) Eine neue Antilope und andere Säugetierreste aus dem Obermiozän Niederösterreichs. Paläobiologica 2:62–88.

Simionescu I, Barbu V (1939) Mamiferele pliocene dela Cimişlia (România). III. Proboscidieni. Acad Rom Public Fondul V Adam 9:1–20.

Stefanescu G (1892) On the existence of the *Dinotherium* in Roumania. Bull Geol Soc Am 3:81–83.

Stehlin HG (1925) Catalogue des ossements de mammifères Tertiaires de la collection Bourgeois à l'École de Pont-Levoy (Loir-et-Cher). Bull Soc hist nat Anthropol Loir-et-Cher 18:77–277.

Steininger F (1965) Ein bemerkenswerter Fund von *Mastodon* (*Bunolophodon*) *longirostris* Kaup 1832 (Proboscidea, Mammalia) aus dem Unterpliozän (Pannon) des Hausruck-Kobernaußerwald-Gebietes in Oberösterreich. Jb Geol Bundesanst 108:195–212.

Stromer E (1938) Huftier-Reste aus dem unterstpliocänen Flinzsande Münchens. Abh Bayer Akad Wiss Math-Naturwiss Abt 44:1–39.
Stromer E (1940) Die jungtertiäre Fauna des Flinzes und des Schweiß-Sandes von München. Nachträge und Berichtigungen. Abh Bayer Akad Wiss Math-naturwiss Abt 48:1–106.
Svistun VI (1974) Dinotheriums of Ukraine. Naukova Dumka, Kiev.
Tassy P (1985) La place des mastodontes Miocènes de l'Ancien Monde dans la phylogénie des Proboscidea (Mammalia): Hypothèses et conjectures. Dissertation, Université Pierre et Marie Curie, Paris.
Tassy P (1986) Nouveaux Elephantoidea (Mammalia) dans le Miocène du Kenya. CNRS, Paris.
Tassy P (1987) A hypothesis on the homology of proboscidean tusks based on paleontological data. Am Mus Novit 2895:1–18.
Tassy P (1990) The "Proboscidean Datum Event": how many proboscideans and how many events? In: Linsday EH, Mein P, Fahlbusch V (eds) European Neogene Mammal Chronology. Plenum Press, New York, pp 237–252.
Tassy P. (1996a) Dental homologies and nomenclature in the Proboscidea. In: Shoshani J, Tassy P (eds) The Proboscidea: Evolution and Palaeoecology of Elephants and their Relatives. Oxford University Press, New York, pp 21–25.
Tassy P (1996b) Growth and sexual dimorphism among Miocene elephantoids: the example of *Gomphotherium angustidens*. In: Shoshani J, Tassy P (eds) The Proboscidea: Evolution and Palaeoecology of Elephants and their Relatives. Oxford University Press, New York, pp 92–100.
Tassy P. (1999) Miocene elephantids (Mammalia) from the emirate of Abu Dhabi, United Arab Emirates: Palaeobiogeographic implications. In: Whybrow PJ, Hill A (eds) Fossil Vertebrates of Arabia. Yale University Press, New Haven and London, pp 209–233.
Tassy P (2013) L'anatomie cranio-mandibulaire de *Gomphotherium angustidens* (Cuvier, 1817) (Proboscidea, Mammalia): données issues du gisement d'En Péjouan (Miocène moyen du Gers, France). Geodiversitas 35:377–445.
Tassy P (2014) L'odontologie de *Gomphotherium angustidens* (Cuvier, 1817) (Proboscidea, Mammalia): données issues du gisement d'En Péjouan (Miocène moyen du Gers, France). Geodiversitas 36:35–115.
Tassy P (2016) Proboscidea. In: Sen S (ed) Late Miocene mammal locality of Küçükçekmece, European Turkey. Geodiversitas 38(2):261–271.
Thenius E (1952) Die Säugetierreste aus dem Jungtertiär des Hausruck und Kobernaußerwaldes (O.-Österr.) und die Alterstellung der Fundschichten. Jb Geol Bundesanst Wien 95:119–144.
Tobien H (1973) On the evolution of mastodonts (Proboscidea, Mammalia). Part I: The bunodont trilophodont groups. Notizbl hess Landesamt Bodenforsch 101:202–276.
Tobien H (1978) On the evolution of mastodonts (Proboscidea, Mammalia). Part 2: The bunodont tetralophodont groups. Geol Jb Hessen 106:159–208.
Tobien H. (1980) A note on the mastodont taxa (Proboscidea, Mammalia) of the "Dinotheriensande" (Upper Miocene, Rheinhessen, Federal Republic of Germany). Mainzer geowiss Mitt 9:187–201.
Tobien H (1988) Contributions a l'etude du gisement miocene superieur de Montredon (Herault). Les grands mammiferes. 7 – les proboscidiens Deinotheriidae. Palaeovertebrata, Mém ext 1988:135–175.
Tobien H (1996) Evolution of zygodons with emphasis on dentition. In: Shoshani J, Tassy P (eds) The Proboscidea: Evolution and Palaeoecology of Elephants and their Relatives. Oxford University Press, New York, pp 76–85.
van der Maarel FH (1932) Contributions to the knowledge of the fossil mammalian fauna of Java. Wet Meded Dienst Mijnb Nederlandsch-Indië 15:1–208.
Vergiev S, Markov GN (2012) Fossil proboscideans (Mammalia) from the collections of the Varna Regional Museum of History. Acta Zool Bulg 64:427–438.
von Meyer H (1831) Mittheilung an geheimen Rath von Leonhard. Jb Min Geogn Geol Petrefaktenkunde 2:296–297.
Voorhies MR (1969) Taphonomy and population dynamics of an early Pliocene vertebrate fauna, Knox County, Nebraska. Rocky Mt Geol 8:1–69.
Wagner A (1848) Urweltliche Säugthier-Ueberreste aus Griechenland. Abh Bayer Akad Wiss 5:335–378.
Wagner A (1857) Neue Beiträge zur Kenntnis der fossilen Säugthier-Ueberreste von Pikermi. Abh Bayer Akad Wiss 8:109–158.
Xafis A, Saarinen J, Bastl K, Nagel D, Grímsson F (2020) Palaeodietary traits of large mammals from the middle Miocene of Gračanica (Bugojno Basin, Bosnia-Herzegovina). Palaeobiodivers Palaeoenviron 100:457–477.

Terms and Conditions

Springer Nature journal content, brought to you courtesy of Springer Nature Customer Service Center GmbH (“Springer Nature”).
Springer Nature supports a reasonable amount of sharing of research papers by authors, subscribers and authorised users (“Users”), for small-scale personal, non-commercial use provided that all copyright, trade and service marks and other proprietary notices are maintained. By accessing, sharing, receiving or otherwise using the Springer Nature journal content you agree to these terms of use (“Terms”). For these purposes, Springer Nature considers academic use (by researchers and students) to be non-commercial.
These Terms are supplementary and will apply in addition to any applicable website terms and conditions, a relevant site licence or a personal subscription. These Terms will prevail over any conflict or ambiguity with regards to the relevant terms, a site licence or a personal subscription (to the extent of the conflict or ambiguity only). For Creative Commons-licensed articles, the terms of the Creative Commons license used will apply.
We collect and use personal data to provide access to the Springer Nature journal content. We may also use these personal data internally within ResearchGate and Springer Nature and as agreed share it, in an anonymised way, for purposes of tracking, analysis and reporting. We will not otherwise disclose your personal data outside the ResearchGate or the Springer Nature group of companies unless we have your permission as detailed in the Privacy Policy.
While Users may use the Springer Nature journal content for small scale, personal non-commercial use, it is important to note that Users may not:

1. use such content for the purpose of providing other users with access on a regular or large scale basis or as a means to circumvent access control;
2. use such content where to do so would be considered a criminal or statutory offence in any jurisdiction, or gives rise to civil liability, or is otherwise unlawful;
3. falsely or misleadingly imply or suggest endorsement, approval , sponsorship, or association unless explicitly agreed to by Springer Nature in writing;
4. use bots or other automated methods to access the content or redirect messages
5. override any security feature or exclusionary protocol; or
6. share the content in order to create substitute for Springer Nature products or services or a systematic database of Springer Nature journal content.

In line with the restriction against commercial use, Springer Nature does not permit the creation of a product or service that creates revenue, royalties, rent or income from our content or its inclusion as part of a paid for service or for other commercial gain. Springer Nature journal content cannot be used for inter-library loans and librarians may not upload Springer Nature journal content on a large scale into their, or any other, institutional repository.
These terms of use are reviewed regularly and may be amended at any time. Springer Nature is not obligated to publish any information or content on this website and may remove it or features or functionality at our sole discretion, at any time with or without notice. Springer Nature may revoke this licence to you at any time and remove access to any copies of the Springer Nature journal content which have been saved.
To the fullest extent permitted by law, Springer Nature makes no warranties, representations or guarantees to Users, either express or implied with respect to the Springer nature journal content and all parties disclaim and waive any implied warranties or warranties imposed by law, including merchantability or fitness for any particular purpose.
Please note that these rights do not automatically extend to content, data or other material published by Springer Nature that may be licensed from third parties.
If you would like to use or distribute our Springer Nature journal content to a wider audience or on a regular basis or in any other manner not expressly permitted by these Terms, please contact Springer Nature at

onlineservice@springernature.com